1-1-1967

Theoretical analysis of biaxially loaded beam-columns.

Thomas Lawrence Scott
University of Windsor

THEORETICAL ANALYSIS OF BIAXIALLY LOADED BEAM-COLUMNS

A Thesis
Submitted to the Faculty of Graduate Studies through the
Department of Civil Engineering in Partial Fulfilment
of the Requirements for the Degree of
Master of Applied Science at the
University of Windsor

by

Thomas Lawrence Scott

B.A.Sc., University of Windsor, 1966

Windsor, Ontario
1967

ABK 3448

Approved By: W. North

G. Abdel-Sayed

177162 W. McVinnie

ABSTRACT

This study is an analytical investigation of the behaviour of biaxially loaded, simply-supported, beam-columns. Although the analysis is, in general, applicable to any type of cross section, only solid rectangular cross sections of an elastic-plastic material are considered. Equal end moments or moments at one end only are applied to a column having a constant axial load and moment-deflection curves are developed. An IBM 1620 computer is used to make all the necessary calculations. A limited number of tests were performed to substantiate the theoretical solution.

Parameters investigated include the slenderness ratio, cross-sectional shape of the column, the ratio of the end moments applied at the same end, and the ratio of the moments applied at each end. Because of the large number of possible combinations of parameters, only a limited range of these parameters was studied.

It was determined that an increase in minor principle axis bending moment substantially reduces the column's ability to carry major principal axis bending moment for a given slenderness ratio and load. Interaction curves for the biaxially loaded column can be developed for use in the design of such members.

ACKNOWLEDGMENTS

This thesis was prepared under the direction of Dr. William W. McVinnie, to whom the writer wishes to express his appreciation for the assistance given.

The author wishes to thank the Computer Center at the University of Windsor for making its facilities available for use in this investigation and also Mr. George Michalczuk for his technical assistance in preparing the test specimens.

Financial assistance for this project was provided by the National Research Council of Canada.

TABLE OF CONTENTS

LIST OF FIGURES

LIST OF TABLES

CHAPTER I - INTRODUCTION

1.1 Object and Scope

In recent years a considerable amount of work has appeared concerning the behaviour of columns subjected to moments applied about one principle axis of the cross section. This approximates the type of loading which would occur in plane frames. The study of such beam-column behaviour presents a formidable problem because of the necessity of considering inelastic action. Buildings are of necessity three dimensional, but are normally analyzed as a series of plane frames. However, interaction between planes results in some members being acted upon by loads from more than one plane. For example, corner columns of such frames might well be subjected to biaxial moment, i.e., a moment about each of the principal axes of the cross section. Since little research has been done on the behaviour of columns loaded in such a manner, particularily when inelastic action occurs, the object of this research is to develop an analysis to study biaxially loaded beam-columns.

In order to facilitate the investigation, computer programs were developed to do all the numerical work. To limit the scope of the analysis, only columns with moment applied at one end, or equal moments applied at both ends, were considered. In the latter case, the moments may cause either single or double curvature of the column. Further,

only a solid rectangular cross section was used in this investigation; however, the analysis can readily be extended to columns with other cross sections.

1.2 General Comments

The expression "beam-column" refers to a member which is simultaneously subjected to an axial load and bending moments. The bending moments may result from known eccentricities of the axial load or from transverse loading. As the bending moment approaches zero, the member tends to become a centrally loaded column and when the axial force approaches zero, the problem becomes that of a beam.

If an eccentrically loaded column were to remain elastic, its behaviour could be represented by a load-deflection curve, which becomes asymptotic to the Euler load (Fig. 1.1), where the Euler load is given by

$$P_e = \frac{\pi^2 EI}{L^2}$$

and P_e = Euler load

E = Modulus of Elasticity for the column material

I = Moment of Inertia of the column cross section

L = effective column length

However, this behaviour is impossible since the column becomes inelastic at a value of the load less than P_e and the result is a load-deflection curve which is similar to that shown in Fig. 1.2. The collapse load represented by

this curve is normally some what less than the Euler load. As the load is increased beyond initial yielding, plastification progresses along and across the column, thereby reducing its resistance to further loading. In Fig. 1.2, the portion of the curve from O to A represents the column behaviour when the stresses are still elastic. The portion from A to B represents the range of partial yielding. Finally, when the curve reaches point B, a further increase in load becomes impossible because the internal stiffness of the column is just enough to resist the applied load and moment. It is evident that this type of failure occurs by virtue of excessive bending in the plane of the applied moment.

If the member is subjected to bending about the stronger of its two principal axes, and if no lateral support is provided, the column may twist and bend out of the plane of loading and failure occurs due to lateral-torsional buckling. This has the effect of reducing the collapse load from that shown in Fig. 1.2.

The behaviour of the biaxially loaded column is represented by a curve similar to that of Fig. 1.2. In this case, however, the determination of deflection plotted in this figure becomes more complex than for the unaxially loaded column and, as a result, the determination of the collapse load also becomes much more complex. This is due to the fact that three interdependent displacements of the column cross section must be considered. These are lateral

displacements in the two directions and a rotation of the section about its center of twist.

1.3 Previous Investigations

1.3.1 Single Axis Bending

A number of studies and reviews of the beam-column problem for single axis bending have been made. Early developments, including the work of von Karman, Ros and Brunner, Chwulla, Westergaard and Osgood, Jezek and others, have been reviewed in an extensive resume by Bleich (4). Recent work has extended the investigation of the early researchers in the field of eccentrically loaded columns. This has been stimulated by the increasing use of plastic methods of design (1,5,11).

Newmark(15) presented an iterative numerical technique in which external moments were found from an assumed deflection curve and a new deflection curve was calculated by numerical integration using the internal moment-curvature relation. The process was continued until the correct shape was reached as indicated by compatible external and internal conditions.

Applications of the Newmark procedure in determining load-deflection curves of wide flange columns have been made by Ketter, Kaminsky, and Beedle(12) and Galambos and Ketter (9). In these works, a length, load, and end moment are assumed and a deflected shape determined. By varying the end moment, a plot of end moment versus rotation can be

made to determine the maximum end moment for the particular length and axial load. If the process is repeated many times for other lengths and loads, the final results can be presented on an interaction diagram of load versus critical moment for constant length. It should be noted that the results are good only for a specified load-moment-curvature relation, as determined by the cross section and material. The theoretical solutions given in these investigations were compared to tests by Mason, Fisher and Winter (13).

A slight variation of the method just outlined is used by Huber and Ketter(10). Instead of fixing the length, the axial load and end moment are fixed and the length which produces a given center deflection is found by the iterative technique. In this procedure a plot of length versus deflection will indicate the critical length which will support the loads. A definite advantage of specifying the load rather than the length is that the iteration will always converge to give a length when the loads are specified. Convergence will not occur when the length is specified if the load selected is higher than the critical load for that length.

Most analyses of beam-columns have been concerned with the isolated member subjected to single axis bending, whereas practical beam-columns are usually a part of a frame. Recent research(5,11) has given increasing attention to the behaviour of complete frames and to the effects of end

restraint on beam-column behaviour. Ellis and Ojalvo (6,16) have both presented general techniques that will work for unequal end moment and end restraint. A key device used by both authors is the column deflection curve, which is the shape a column will take if the axial load and deformation at a certain point are specified. Ellis determines the shapes of the curves by using differential equations while Ojalvo uses a direct integration procedure outlined by Timoshenko (19). A semi-graphical procedure is used by Ellis to find the portions of the curve which represent failure struts. Ojalvo uses another semi-graphical procedure and known boundary conditions to find the portion of a curve that represents a given column. By using several curves, a load versus deformation history can be plotted to find the critical load. Bijlaard (2) uses a somewhat similar procedure with the simplifying assumption that the deflection curve is a sine wave. The work involved in any of the methods of finding critical loads of restaint columns is considerably reduced if the member is symmetric. However, graphical or trial procedures must still be used.

1.3.2 Biaxial Bending

The analytical study of the biaxially loaded beam-column, both isolated and as an integral part of the building frame, has only recently been attempted. This is because of the much more complex nature of this problem compared with that of single axis bending, since three interdependent displacements are now needed to describe the column behaviour.

Birnstiel and Michalos (3) have presented an analysis of biaxially loaded wide flange columns. In this analysis, the column is divided into a number of panels. Values of the second derivatives of the three displacements are assumed at each panel point, and a trial equilibrium position is determined by numerical integration. The values of the curvatures and the second derivatives of the angle of twist are adjusted until equilibrium between external and internal forces and moments is established at each panel point. Internal moments and forces are found by dividing the cross section into a number of elements by a rectangular grid, determining the strain on each element, and summing the results over all the elements of the cross section. By assuming increasing values of the second derivatives of the displacements, a curve of load versus deflection is obtained, which leads directly to the collapse load of the column. In their paper, only columns which are symmetric about midheight are considered.

Sharma (18) has presented an approximate method for determining the ultimate load of columns having the same eccentricity of loading at each end. The basis of this procedure is the assumption that the lateral and twisting displacements vary sinusoidally along the column. At midheight, a value of the second derivative of one of the lateral displacements is specified, and equilibrium between internal and external forces and moments is established.

Knowing the displacement at midheight thus determines the deflected shape of the column. By incrementing the specified second derivative, a load-deflection curve is obtained. Comparison of the theoretical results with a large number of test results showed good agreement.

Ellis (7, 8) determines the ultimate carrying capacity of biaxially loaded columns by use of the overlapping shape failure criterion (6). Briefly, this criterion requires that two intersecting column deflection curves be determined so that a column on the verge of collapse has been defined; since, between the points of intersection, two column shapes exist for the same axial load and end conditions. Column deflection curves are found only for a square tubular section. Since this type of cross section is torsionally stiff, twisting displacements are neglected and thus only two deflections at any point along the column need to be determined. These deflections are found by consideration of a short element which is systematically subjected to rotations about each principal axis for a specified axial load, and the axial strain and bending moments are determined for each combination. This information is then used to numerically integrate for the deflected shape.

McVinnie (14) considered the analytical study of a biaxially loaded column as an integral part of a simple orthogonal space frame subjected to symmetrical vertical loading. Moment-thrust-curvature curves were set up and

numerical integration yielded column deflection curves for rectangular tubular columns, neglecting twist. Since this procedure forms the basis for the analytical study in this thesis, it will be closely examined in the next chapter.

A review of the literature on the experimental investigation of biaxially loaded columns is given in References 3 and 18. Most of these experimental results are for columns having equal eccentricities at each end with the cross section being either wide flange, I, or channel. Some interesting tests have been presented by Baker(1) in which biaxially loaded columns in laterally braced frames were simulated by loading the test specimens through elastic beams framing at right angles into each end of the column and by an axial force applied to the specimen. Solid rectangular and wide flange sections were considered but no attempt at an analytical solution was given.

CHAPTER II - THEORETICAL SOLUTION

2.1 Description of the Problem

The biaxially loaded beam column under investigation (Fig. 2.1) is of length L and simply supported at each end, i.e., displacements are zero but rotations are permitted about the x and y axes. The loading is such that the axial load, P, is applied to the column and then end moments about the x and y axes are increased simultaneously to collapse. In this study, moments are designated as M^x or M^y where the superscript indicates the axes about which they act. Subscripts are used to designate position of the moment. For example, M^x_A is the moment about the x-axis at point A in Fig. 2.1. To further define the loading, the ratio of x-moment to y-moment at the ends of the column is designated as α and a constant β is defined as the ratio of the x-moment at B to the x-moment at A. The ratios β and α are considered to remain constant throughout the loading. As noted previously, only values of β of zero and one are considered in this study.

A solid rectangular cross section is used throughout this investigation (Fig. 2.2). The half depth of the cross section is taken as D, the half width as KD, and the x and y axes are oriented in the same sense as those of Fig. 2.1.

2.2 Method of Solution

The analysis presented herein involves the determination of moment-deflection curves such as those shown in Figs. 2.7

and 2.10. The ordinate of the curve may be any of the end moments since all are related by β and γ. For a given column, P, ϵ, and γ are specified and the end moments increased until the peak moment on the moment-deflection curve is obtained. A typical point on this curve is found from the column deflection curve which is the shape a column will take if the load and deformation at a point are specified. A numerical integration procedure presented by McVinnie (14) is used to develop the column deflection curve. By consideration of many specific problems, interaction curves for the biaxially loaded column can be developed.

2.3 Assumptions

In this study, the following assumptions are made:

1) Deflections and rotations are small in accordance with small deflection theory.

2) Deflections occur in the x and y directions only, no twisting of the column is allowed.

3) Plane sections before bending remain plane after bending.

4) The material is mild structural steel which is assumed to have an elastic, perfectly plastic, stress-strain curve (Fig. 2.3). It is further assumed that the tension and compression stress-strain curves are identical. This curve is typical of mild steels, provided that strains no greater than about ten times the yield strain are considered.

5) No unloading occurs in yielded portions of the column.

6) Residual stresses are neglected.

7) Members are originally straight and prismatic.

8) Axial shortening of the column is neglected.

9) The effect of shear on the bending resistance of the cross section is neglected.

2.4 Column Integration

2.4.1 Governing Differential Equations

For the biaxially loaded beam column, the displacements of the cross section at any point along the column are defined by the lateral displacements of the shear center in the x and y directions, u and v respectively, and by the rotation of the section about its shear center. Differential equations of equilibrium for this problem have been derived by Timoshenko and Gere (19). Since the section chosen for this study has considerable torsional stiffness, it is assumed that the rotation of the section and all its derivatives are zero. The governing differential equations then reduce to

$$B^y \frac{d^2u}{dz^2} + P u + C_1 z + C_2 = 0 \qquad (2.1)$$

$$B^x \frac{d^2v}{dz^2} + P v + C_3 z + C_4 = 0 \qquad (2.2)$$

where B^x, B^y = bending stiffnesses about the x and y axes.

z = coordinate along the member.

C_1, C_2, C_3, C_4 = constants of integration.

For the elastic case, where the bending stiffnesses are independent and constant, Eqs. 2.1 and 2.2 are

independent and define the behaviour of the column in the y-z and x-z planes respectively. However, after inelastic action begins, the bending stiffnesses depend upon the extent and position of yielded material which in turn is dependent upon the axial load, applied moments, and the lateral displacements. As a result, Eqs. 2.1 and 2.2 are coupled through these stiffnesses and u and v must be determined simultaneously using a numerical integration procedure.

2.4.2 Numerical Integration Procedure

A typical element of length "a" of the column deflection curve is shown in Fig. 2.4. The x and y displacements at i are denoted by u_i and v_i respectively and those at i+1 by u_{i+1} and v_{i+1}. A projection of the element of Fig. 2.4 onto the y-z plane is shown in Fig. 2.5(a). In this figure, θ^x_i and θ^x_{i+1} are the slopes of the column deflection curve at i and i+1 respectively, ψ^x is the change in slope between i and i+1 and δv is the deflection of i+1 from the tangent to the column deflection curve at i. Assuming that the projection of the element onto the y-z plane is a flat circular arc, δv is given by

$$\delta v = \frac{a}{2} \tan \psi^x \qquad (2.3)$$

Since ψ^x is a small angle,

$$\tan \psi^x = \psi^x = a\, \phi^x_i$$

and

$$\delta v = \frac{a^2}{2} \phi^x_i \qquad (2.4)$$

where ϕ^x_i is the x-axis curvature at i.

From geometry, the deflection at i+1 in the y-direction is

$$v_{i+1} = v_i + a \sin \theta^x_i - \delta v \cos \theta^x_i \qquad (2.5)$$

and the slope of the deflected curve at i+1 is

$$\theta^x_{i+1} = \theta^x_i - \psi^x \qquad (2.6)$$

By considering the projection of the element onto the x-z plane, Fig. 2.5(b), it can be shown that

$$u_{i+1} = u_i + a \sin \theta^y_i - \delta u \cos \theta^y_i \qquad (2.7)$$

$$\theta^y_{i+1} = \theta^y_i - \psi^y \qquad (2.8)$$

Substituting for $\delta v, \psi^x, \delta u$ and ψ^y and making the assumption that θ^x_i and θ^y_i are small angles, the equations for the displacements and rotations at i+1 in terms of those at i are written as

$$v_{i+1} = v_i + a\,\theta^x_i - \frac{a^2}{2}\,\phi^x_i \qquad (2.9)$$

$$u_{i+1} = u_i + a\,\theta^y_i - \frac{a^2}{2}\,\phi^y_i \qquad (2.10)$$

$$\theta^x_{i+1} = \theta^x_i - a\,\phi^x_i \qquad (2.11)$$

$$\theta^y_{i+1} = \theta^y_i - a\,\phi^y_i \qquad (2.12)$$

At this point it is convenient to introduce certain quantities which are used to put Eqs. 2.9 to 2.12 into dimensionless form. These quantities are

$$P_y = \text{yield load} = 4E\epsilon_y KD^2$$

$$M^x_y = \text{yield moment} = \frac{4}{3} E\epsilon_y KD^3$$

$$\phi^x_y = \text{yield curvature} = \epsilon_y/D$$

$$\theta^x_y = \frac{\pi}{3}\sqrt{\epsilon_y/3}$$

where ϵ_y is the yield strain of the material and θ^x_y is the rotation caused by a moment of magnitude M^x_y acting at one end of a simply supported beam of length $\pi D/\sqrt{\epsilon_y * 3}$.

Using these quantities, Eqs. 2.9 to 2.12 are written in dimensionless form as

$$\frac{v_{i+1}}{D} = \frac{v_i}{D} + \frac{a}{D}\frac{\pi}{3}\sqrt{\frac{\epsilon_y}{3}}\frac{\theta^x{}_i}{\theta^x{}_y} - \frac{\epsilon_y}{2}\left(\frac{a}{D}\right)^2\frac{\phi^x{}_i}{\phi^x{}_y} \tag{2.13}$$

$$\frac{u_{i+1}}{D} = \frac{u_i}{D} + \frac{a}{D}\frac{\pi}{3}\sqrt{\frac{\epsilon_y}{3}}\frac{\theta^y{}_i}{\theta^x{}_y} - \frac{\epsilon_y}{2}\left(\frac{a}{D}\right)^2\frac{\phi^y{}_i}{\phi^x{}_y} \tag{2.14}$$

$$\frac{\theta^x{}_{i+1}}{\theta^x{}_y} = \frac{\theta^x{}_i}{\theta^x{}_y} - \frac{3}{\pi}\frac{a}{D}\sqrt{3\epsilon_y}\frac{\phi^x{}_i}{\phi^x{}_y} \tag{2.15}$$

$$\frac{\theta^y{}_{i+1}}{\theta^x{}_y} = \frac{\theta^y{}_i}{\theta^x{}_y} - \frac{3}{\pi}\frac{a}{D}\sqrt{3\epsilon_y}\frac{\phi^y{}_i}{\phi^x{}_y} \tag{2.16}$$

It should be noted that the panel length "a" is now expressed in terms of D.

At any point on a column deflection curve (Fig. 2.4)

$$M^y = P\,u$$

$$M^x = P\,v$$

To construct the curve, the displacements (including rotations) are specified at a point such as B, the moments calculated, and the curvatures found by the procedure given in Section 2.5. Deflections and rotations at the next panel point are calculated using Eqs. 2.13 to 2.16, where the subscript "i" corresponds to point B. Once the deflections at i+1 are found, this point becomes the point i and the procedure is repeated to find the deflections at the next panel point. This process is continued until the desired column length is reached. The accuracy of the deflections at i+1 is increased by first obtaining the deflections at i+1 assuming that the curvatures at i are constant from i to i+1. Using these deflections at i+1, curvatures at this

point are determined and a second set of deflections at i+1 calculated, using the average of the curvatures at i and i+1.

The part of the column deflection curve (Fig. 2.4) between A and B represents the deflected shape of the column shown in Fig. 2.1 provided that the moments at A and B in both figures are the same. To obtain column deflection curves that are readily usable in this study requires a proper selection of initial conditions. For columns having moments applied only at A ($\beta = 0$), the point B is selected to have zero u and v displacements and a combination of rotations, θ^x_B and θ^y_B. For a specified θ^x_B, θ^y_B is found such that the combination would give a moment ratio at A equal to γ if the column were to remain elastic. The resulting column deflection curve is shown in Fig. 2.6. If the calculated ratio, M^y_A/M^x_A, is equal to the specified γ , plus or minus a fixed amount of error, a permissible end moment has been determined and one point on the moment-deflection curve obtained. If the calculated ratio is not equal to γ , plus or minus a fixed amount of error, θ^y_B is corrected and a new column deflection curve found.

The specified θ^x_B is incremented by trial and error so that sufficient points on the moment-deflection curve are obtained. Corrections to θ^y_B are explained using the curve shown in Fig. 2.8. The problem is to find a value of θ^y_B which, when combined with the specified θ^x_B, will give a moment ratio sufficiently close to the specified ratio, γ .

This is accomplished by approximating the curve by a series of secants. Initially the point a on the curve is calculated using the value of θ^y_{B1} obtained from elastic theory. A new point d is calculated from a rotation θ^y_{B2} which is found by extending the secant oa until it intersects the value γ at point c. If necessary, a third approximation is made using the extended secant ad which results in rotation θ^y_{B3} and the point f on the curve. This process is repeated until the desired accuracy is reached or until the slope of the secant becomes negative, a negative slope indicating that the curve has reached a maximum moment ratio below the value γ. In the latter case, it is evident that, for the specified θ^x_B, no value of θ^y_B can be found for γ; therefore, θ^x_B must be decreased. It should be noted that in many cases the first approximation to θ^y_B resulted in a moment ratio sufficiently close to γ.

In studying columns with equal end moments ($\varrho = 1$), use is made of the symmetry of the column deflections about midheight. In this case, the column deflection curve is symmetric and consequently only half the curve needs to be considered. The integration is started at point C (Fig. 2.9) with zero rotations and a combination of displacements, u_C and v_C. These displacements play the same role as θ^x_B and θ^y_B for the case where $\varrho = 0$, and the moment-deflection curve (Fig. 2.10) is constructed in a similar manner.

2.5 Load - Moment - Curvature Relationship

2.5.1 General Procedure

The procedure given in Section 2.4 requires that a relationship between moments and curvatures be determined for a constant axial load and specific cross section. This relationship can be represented by the curves shown in Figs. 2.11 and 2.12. Each of the curves of Fig. 2.11 represents the variation of M^x with ϕ^x for constant values of ϕ^y while those of Fig. 2.12 represent the variation of M^y with ϕ^y for constant values of ϕ^x. The development and use of these curves is considered in the following paragraphs and specific equations for the rectangular cross section are given in Section 2.5.2.

Assuming that plane sections remain plane, the normal strain on a cross section at any point (x,y) may be written as

$$\epsilon = \phi^x y + \phi^y x + \epsilon_o \qquad (2.17)$$

where ϵ_o is a uniform normal strain and ϕ^x and ϕ^y are the curvatures about the x and y axes respectively. With reference to the stress-strain curve of Fig. 2.3, the corresponding stress distribution is

$$\sigma = E\epsilon - E[\epsilon \pm \epsilon_y] \qquad (2.18)$$

The brackets have the significance that when the absolute value of ϵ is less than ϵ_y, the term in the brackets is zero. When ϵ is negative, the plus sign is used for the term inside the brackets and when ϵ is positive, the negative sign

is used for the term inside the brackets.

For the equilibrium of the cross section

$$P = \int_A \sigma \, dA \tag{2.19}$$

Combining Eqs. 2.18 and 2.19 gives

$$P = E\int_A \epsilon \, dA - E\int_A \left[\epsilon \pm \epsilon_y\right] dA \tag{2.20}$$

Similar expressions for the moments are given by Eqs. 2.21 and 2.22

$$M^x = E\int_A y\epsilon \, dA - E\int_A y\left[\epsilon \pm \epsilon_y\right] dA \tag{2.21}$$

$$M^y = E\int_A x\epsilon \, dA - E\int_A x\left[\epsilon \pm \epsilon_y\right] dA \tag{2.22}$$

In Eqs. 2.20 to 2.22, the first integral gives the value of the load or moment if the section were everywhere elastic and the second integral is considered a correction to account for yielding of the cross section, and as such its value will depend on the amount and position of yielding.

There are ten possible yield configurations for the solid rectangular section (Fig. 2.13) and for each, Eqs. 2.20 to 2.22 have forms in terms of the specified values of the section dimensions, P, Φ^x, Φ^y, and ϵ_o. Using these equations, the curves of Figs. 2.11 and 2.12 are developed in the following manner:

1) For a given value of P, the curvatures, Φ^x and Φ^y are specified, leaving ϵ_o the only unknown in Eq. 2.17.
2) Using Eq. 2.20, a value of ϵ_o is determined that corresponds to the specified Φ^x, Φ^y, P, and an assumed yield configuration . It is necessary to assume a yield configuration because of the different form of Eq. 2.20 for each configuration. The yield configuration that

corresponds to the calculated ϵ_o is found and compared to the one assumed. If these are the same, then ϵ_o has been determined. If they are not the same, a new configuration must be assumed and a new value of ϵ_o calculated. The magnitudes of the bending strains at the corners of the section control the sequence of assumed yield configurations. Fig. 2.14 shows the sequence used in this study.

3) When ϵ_o is finally determined, Eqs. 2.21 and 2.22 are used to find M^x and M^y.

4) By varying Φ^x and Φ^y systematically over the desired range of curvatures, the required curves are determined.

The curves of Figs. 2.11 and 2.12 are developed for the load under consideration before the numerical integration is begun. Using these curves, the values of the curvatures for any combination of M^x and M^y are determined as follows:

1) For any value of M^x (for example, M^x_o), the combinations of curvatures resulting in this moment are found at the intersections of M^x_o with the constant Φ^y curves of Fig. 2.11. A plot of these intersections is shown as curve A in Fig. 2.15.

2) For any value of M^y (for example, M^y_o), the combinations of curvatures resulting in this moment are found at the intersections of M^y_o with the constant Φ^x curves of Fig. 2.12. A plot of these intersections is shown as curve B in Fig. 2.15.

3) The resulting curvatures for M^x_o and M^y_o acting together are determined by the intersection of curve A (step 1)

with curve B (step 2). These are designated as Φ^x_o and Φ^y_o in Fig. 2.15.

2.5.2 Development of the Load - Moment - Curvature Equations

The load-moment-curvature relationship for the solid cross section is developed from Eqs. 2.20, 2.21 and 2.22. Dividing these equations by the appropriate factors given in Section 2.4 results in dimensionless equations,

$$\frac{P}{P_y} = \frac{D^2}{A}\int_A \frac{\epsilon}{\epsilon_y}\frac{dA}{D^2} - \frac{D^2}{A}\int_A \left[\frac{\epsilon}{\epsilon_y} \pm 1\right]\frac{dA}{D^2} \qquad (2.23)$$

$$\frac{M^x}{M^x_y} = \frac{D^4}{I^x}\int_A \frac{y}{D}\frac{\epsilon}{\epsilon_y}\frac{dA}{D^2} - \frac{D^4}{I^x}\int_A \frac{y}{D}\left[\frac{\epsilon}{\epsilon_y} \pm 1\right]\frac{dA}{D^2} \qquad (2.24)$$

$$\frac{M^y}{M^x_y} = \frac{D^4}{I^x}\int_A \frac{x}{D}\frac{\epsilon}{\epsilon_y}\frac{dA}{D^2} - \frac{D^4}{I^x}\int_A \frac{x}{D}\left[\frac{\epsilon}{\epsilon_y} \pm 1\right]\frac{dA}{D^2} \qquad (2.25)$$

where $A\ (=4KD^2)$ = the area of the cross section.

$I^x(=4/3\ KD^4)$ = the moment of interia of the cross section about the x-axis.

The first integral in each equation represents the volume (or the first moment of the volume) of the ϵ/ϵ_y distribution (Fig. 2.16) and may be written as

$$\frac{D^2}{A}\int_A \frac{\epsilon}{\epsilon_y}\frac{dA}{D^2} = \frac{\epsilon_o}{\epsilon_y}$$

$$\frac{D^4}{I^x}\int_A \frac{y}{D}\frac{\epsilon}{\epsilon_y}\frac{dA}{D^2} = \frac{\Phi^x}{\Phi^x_y}$$

$$\frac{D^4}{I^x}\int_A \frac{x}{D}\frac{\epsilon}{\epsilon_y}\frac{dA}{D^2} = \frac{I^y}{I^x}\frac{\Phi^y}{\Phi^x_y}$$

where $I^y(=4/3\ K^3D^4)$ = the moment of interia of the cross section about the y-axis.

The second integral in each equilibrium equation is the

volume (or the first moment of the volume) of the $\left[\frac{\epsilon}{\epsilon_y} \pm 1\right]$ distribution. For each of the ten possible yield configurations of Fig. 2.13, the required volume (or moment of the volume) can be obtained from an appropriate combination of the three volumes of Fig. 2.17. The "a" dimensions (Fig. 2.17) represent values of $\left[\frac{\epsilon}{\epsilon_y} \pm 1\right]$ and the "c" dimensions represent lengths of yielding along the edges and can be written in terms of the strains at the corners of the cross section. A typical edge is shown in Fig. 2.18, where i or j take the values 1, 2, 3, and 4 depending on the position of the edge in the cross section (Fig. 2.16). The strain at end i is taken as the algebraically largest strain on the edge. The length of the tension and/or compression yield on a side, $a_{ij}K_1D$ and/or $a_{ji}K_1D$, is found by proportion to be

$$a_{ij}K_1D = \frac{2(\epsilon_i/\epsilon_y - 1)}{(\epsilon_i/\epsilon_y - \epsilon_j/\epsilon_y)} K_1D \qquad (2.26)$$

$$a_{ji}K_1D = -\frac{2(\epsilon_j/\epsilon_y + 1)}{(\epsilon_i/\epsilon_y - \epsilon_j/\epsilon_y)} K_1D \qquad (2.27)$$

where K_1 is one or K, depending on the edge considered.

The strain at any point (x,y) in terms of the yield strain is given by Eq. 2.17 divided by ϵ_y and with x and y expressed in terms of D.

$$\frac{\epsilon}{\epsilon_y} = \frac{y}{D}\frac{\phi^x}{\phi^x_y} + \frac{x}{D}\frac{\phi^y}{\phi^x_y} + \frac{\epsilon_o}{\epsilon_y} \qquad (2.28)$$

The first two terms on the right hand side represent "bending strains" and depend only on the values of the curvatures and the section dimensions. The third term depends on the magnitude

of the axial load. The strain at any corner is found by substituting the coordinates of the corner into Eq. 2.28. Using $\bar{\epsilon}_i$ to represent the "bending strains" at i and $\bar{\epsilon}_j$ to represent those at j, Eqs. 2.26 and 2.27 can be written as

$$a_{ij}K_1D = \frac{(\bar{\epsilon}_i/\epsilon_y - 1) + \epsilon_o/\epsilon_y}{\phi^x / \phi^x_y} K_1D \qquad (2.29)$$

$$a_{ji}K_1D = -\frac{(\bar{\epsilon}_j/\epsilon_y + 1) - \epsilon_o/\epsilon_y}{K\,\phi^y / \phi^x_y} K_1D \qquad (2.30)$$

The Eqs. 2.29 and 2.30 are used to express the "c" dimensions of Fig. 2.17 in terms of the strains, curvatures and section dimensions. Once this has been done for any yield configuration, the volume calculations are straightforward. The final expressions used for Eqs. 2.23, 2.24 and 2.25 are given in Tables 2.1, 2.2 and 2.3. It should be noted that the expressions are independent of D and ϵ_y.

The equations given in Table 2.1 are used to calculate ϵ_o/ϵ_y for given values of P/P_y, ϕ^x/ϕ^x_y, ϕ^y/ϕ^x_y and K. These equations reduce to the three types

$$\frac{P}{P_y} = a\left(\frac{\epsilon_o}{\epsilon_y}\right) + b \qquad (2.31)$$

$$\frac{P}{P_y} = a\left(\frac{\epsilon_o}{\epsilon_y}\right)^2 + b\left(\frac{\epsilon_o}{\epsilon_y}\right) + c \qquad (2.32)$$

$$\frac{P}{P_y} = a\left(\frac{\epsilon_o}{\epsilon_y}\right)^3 + b\left(\frac{\epsilon_o}{\epsilon_y}\right)^2 + c\left(\frac{\epsilon_o}{\epsilon_y}\right) + d \qquad (2.33)$$

where a, b, c and d are coefficients that depend only on the cross-sectional dimensions and the particular values of ϕ^x/ϕ^x_y and ϕ^y/ϕ^x_y selected, and as such are constant.

The solution of Eq. 2.31 for ϵ_o/ϵ_y is straightforward. The quadratic equation, Eq. 2.32, is rewritten as

$$a\left(\frac{\epsilon_o}{\epsilon_y}\right)^2 + b\left(\frac{\epsilon_o}{\epsilon_y}\right) + \left(c - \frac{P}{P_y}\right) = 0 \qquad (2.34)$$

The solution to Eq. 2.34 is

$$\frac{\epsilon_o}{\epsilon_y} = \frac{-b + \sqrt{b^2 - 4a\,(c - P/P_y)}}{2a}$$

where the sign on the radical follows from the fact that ϵ_o must increase algebraically with P. The cubic equation, Eq. 2.33, is rearranged to give

$$a\left(\frac{\epsilon_o}{\epsilon_y}\right)^3 + b\left(\frac{\epsilon_o}{\epsilon_y}\right)^2 + c\left(\frac{\epsilon_o}{\epsilon_y}\right) + (d - P/P_y) = 0 \qquad (2.35)$$

The solution to this equation involves solving for one real root, recalculating the coefficients, and solving the resulting quadratic equation for the remaining roots, either real or imaginary. It can be shown that the algebraically smallest real root gives the required value of ϵ_o/ϵ_y.

Once ϵ_o/ϵ_y has been found for the given ϕ^x/ϕ^x_y, ϕ^y/ϕ^x_y, and P/P_y, the moments are found using the appropriate equations from Tables 2.2 and 2.3.

CHAPTER III - COMPUTATIONS

3.1 Computer Programs

An IBM 1620 Mk II computer was used to make all the necessary calculations. Two separate sets of programs were written in Fortran II.

The first set of programs established the constant-curvature, moment curvature curves for the given section, loads and specified values of the curvatures. Subprograms were developed to solve the cubic and quadratic equations for ϵ_o/ϵ_y. Due to the limited capacity of the computer, the program controlling the sequence of assumed yield configurations was divided into two parts; the first part consisting of those cases starting at A and B in Fig. 2.14 and the second part consisting of those starting at C and D. The moment-curvature data from both programs was combined in a third program to give a complete set of data.

In order to check the rather lengthy expressions used in the moment-curvature computations, a program was written which would take the calculated value of ϵ_o along with the specified values of the curvatures and determine the corresponding loads and moments. Essentially this program divided the section into 200 elements. The strain and corresponding stress at the center of each element was found and the contribution of each element to the load and each moment was determined. Total load and moments were calculated by summing the contributions from each element. The load

determined in this manner was checked against the specified load and the moments checked against those calculated from the moment equations. In this manner, a number of programming and derivation errors were discovered which otherwise would have gone unnoticed.

The second set of programs consisted of two independent programs to determined the moment-deflection curve for the case when $\mathcal{C} = 0$ ($\mathcal{C} = -1$) and when $\mathcal{C} = 1$. In both of these programs, a curvature subprogram was used to determine specific values of curvature for the moments calculated at each panel point on the column deflection curve.

Flow diagrams for both sets of programs are given in Figs. 3.1 and 3.2.

3.2 Numerical Calculations

The numerical calculations involved curve interpolation and finding the coordinates of the intersection of two curves.

The curvature subprogram for determining the column deflection curves requires a method of interpolating between specific points on the constant-curvature, moment-curvature curves. For example, the constant moment curves of Fig. 2.15 showing the relationship between Φ^x and Φ^y are found by interpolating from points on the curves of Figs. 2.11 and 2.12. Second-degree polynomials derived from three data points bounding the value of the independent variable were used for all interpolations. These curves have the general shape of most of the curves found in this study, at least over the limited range of three data points.

The curvature determination (Section 2.5.1) requires that the coordinates of the intersection of two curves be found. Two points on each curve are selected and a linear equation is written through each pair. The coordinates of the intersection of these two straight lines are found and compared with the coordinates of the points determining the lines. If the coordinates of the intersection are bounded by the points, an approximation to the intersection has been obtained. If the coordinates of the intersection are not bounded, then a new point on one or both curves is selected and the process repeated. Once the intersection is bounded, a second degree equation is written through the two bounding points plus a third point on each curve. The curves are thus approximated by the equations

$$\phi^{y}_{1} = a\,(\phi^{x}_{1})^{2} + b\,(\phi^{x}_{1}) + c$$

$$\phi^{y}_{2} = d\,(\phi^{x}_{2})^{2} + e\,(\phi^{x}_{2}) + f$$

At the intersection, the following must hold:

$$\phi^{y}_{1} = \phi^{y}_{2}$$

$$\phi^{x}_{1} = \phi^{x}_{2}$$

Equating the two ϕ^{y} values gives a quadratic equation in ϕ^{x}. This is solved using Newton's second order method (17) where the first approximation to the root is given by the linear equations written through each pair of bounding points.

CHAPTER IV - DISCUSSION OF RESULTS

4.1 General Comments

A number of factors affect the behaviour of biaxially loaded columns. Among these are the relative cross-sectional dimensions(K), the slenderness ratio(L/r^y), the ratio of end moments(β), the ratio of the moments at the same end(γ), and the axial load(P). Consideration of all these factors would require the solution of an extremely large number of problems. Since the prime purpose of this study is to develop and program an analysis, and since the rectangular section is not very common, only a limited number of problems were solved.

The solution of a typical problem for the case of $\beta=1$ required 10 to 25 minutes of computer running time, depending on the given load and slenderness ratio. For the case of $\beta=0$, the time required varied from 20 to 55 minutes for each problem. The constant-curvature, moment-curvature curves required about 2 minutes of these times.

Many elastic points on the moment-deflection curves were obtained and served to check the computer programming. In addition, a series of hand computations were made for the square column with $P/P_y=.6$, $L/r^y=100$, $\beta=1$, and $\gamma=1$, in order to check the column integration performed by the computer. The maximum error found by these hand computations was .3%.

In the development of the column deflection curves, the panel length, a, was taken as no more than four times the radius of gyration; exact values were selected to give

slenderness ratios of either 40, 60, 80 or 100. The values of the curvatures (in terms of ϕ^x_y), used to obtain Figs. 2.11 and 2.12, ranged from 0 to 11.

A material having a yield strain of .0011 was used throughout this study except when comparing results with some experimental data, where the yield strain of .0016 was used.

4.2 Numerical Results

4.2.1 Interaction Curves

Interaction curves for the solid rectangular section are shown in Figs. 4.1 and 4.2 for β =1 and β =0. These curves show a non-dimensional plot of the relationship between the axial force and the end bending moment for constant values of the slenderness ratio. As the load is increased, the moment capacity of the column is substantially decreased at all slenderness ratios. The effect of an increase in slenderness is to decrease the load carrying capacity of the column. This decrease is not as pronounced when β =0 (Fig. 4.2) because of the absence of moments at one of the ends. It should be noted that, in this latter case, the reduction in capacity from the zero length column is very small when L/r^y is less than 60. The case β =-1 is represented by Fig. 4.2 with the slenderness ratios doubled, provided that buckling of the column in single curvature does not occur (see page 94 of Reference 5).

4.2.2 Effect of Moment Ratio, α

The effect of α on the moment capacity of various cross-sectional shapes for a given load (P/P_y=.6) and slenderness

ratio(L/r^y) is shown in Figs. 4.3 and 4.4. Since M^x_y depends linearly on K, $K M^x_A/M^x_y$ was plotted as the ordinate so that the four curves in each figure could be compared directly. It can be seen that, as γ increases, the moment capacity of all sections is substantially reduced, particularly for small values of γ. It is also noted that for γ less than about .6 (ρ =1) or .5 (ρ =0), the section having K=.75 carries a larger moment than the larger square section(K=1). This can be explained from the fact that L/r^y is constant for all curves. Since r^y decreases linearly with K, the length of column decreases linearly, as does the slenderness ratio L/r^x. When collapse occurs by bending about the x-axis, as may be the case when γ is small, the smaller L/r^x leads to a higher M^x_A for a given load (Figs. 4.1 and 4.2). Alternatively, as γ decreases, it is possible for failure to occur due to bending about the y-axis. For the extreme case where γ =0, failure in y-axis bending would correspond to lateral buckling of the member. This lateral buckling probably does not occur when K=.75.

4.2.3 Effect of Permissible Error in γ

Since the prime concern of any computer program is the execution time, a study was made to determined the influence of the error in γ on the predicted collapse moments. A small increase in the specified error substantially decreased the time required for the computer to solve a given problem. A very limited study was made by considering a column having

$L/r^{y}=100$, $\beta=1$, $P/P_y=.6$, and $\gamma=.5$. The results are shown in Fig. 4.5 where percent error in γ is plotted versus percent error in moment. For this single case it can be seen that the error in γ, for all sections except K=.25, was greater than the error in moment. Further investigations of other loads and slenderness ratios are needed to substantiate this behaviour. It might be worthwhile to change the order of incrementing displacements to obtain the moment-deflection curves (Section 2.4.2), particularly for the narrow cross sections (small K) or high values of γ.

4.3 Experimental Results

Three small scale tests were performed in order to provide experimental data to compare with theoretical results. These tests were carried out on 3/8 inch square steel specimens having a yield stress of 48 ksi and a yield strain of .0016. A sketch of a typical specimen and loading arrangement is shown in Fig. 4.6. The length of each specimen was selected to give a slenderness ratio of 100. Eccentricities of loading at each end for each of the three specimens corresponded to $\gamma=.5$ and $\beta=1$.

In testing the specimens, the load was increased from zero to collapse. Consequently, the behaviour of each specimen during its loading could not be predicted by the theory presented in this study. The collapse load can be predicted, however, using the interaction curves shown in Fig. 4.7. Curve A represents the column specimen tested, except for the

effect of the end plates. By assuming the end plates to be rigid, curve B, representing the composite of the specimen and the end plates, was determined. It can be shown that the dimensionless load-moment relationship at the end of the specimen is given by

$$\frac{P}{P_y} = \frac{(r^x)^2}{e^x D} \frac{M^x}{M^x_y}$$

where e^x is the eccentricity from the x-axis. This equation is shown as line OC in Fig. 4.7 and its intersection with curve B gives the theoretical collapse load.

The theoretical and experimental results are given in the following table:

Test	e^x in	e^y * in	P(theor.) lbs	P(exp.) lbs	P(exp.)/P(theor.)
1	3/16	3/32	1222	1300	1.06
2	3/8	3/16	810	900	1.11
3	1/2	1/4	675	750	1.11

* e^y is the eccentricity from the y-axis.

It can be seen that the magnitude of the error ranged from 6 to 11 percent. These results are considered to be quite good considering the small scale nature of the tests. It is also possible that unloading may occur in some cases. Unloading would account for the column carrying a larger load than predicted by the theory. If this is the case, the theoretical results should be conservative.

CHAPTER V - CONCLUSIONS AND FUTURE RESEARCH

5.1 Conclusions

An analysis of the biaxially loaded column has been presented which is specifically applicable to the solid rectangular column cross section; however, this analysis can be readily extended to other cross sections.

Although a relatively small amount of data was accumulated in this study, the following conclusions can be made:

1) End moments at collapse are substantially decreased with an increase in slenderness ratio and/or axial load acting on the column.
2) An increase in minor principal axis bending moment (M^y) can substantially reduce the column's ability to carry major principal axis bending moment (M^x) for a given slenderness ratio and axial load.
3) Interaction curves for the biaxially loaded column can be developed for use in the design of such members.
4) The few experimental results show that, over the limited range of the parameters considered, the theory can be used to predict collapse loads with a reasonable degree of accuracy.

5.2 Future Research

To further check the theory, a larger number of tests should be made using rectangular shapes of different relative dimensions. Since only a solid section was considered, future studies should include columns with other shapes, such as

wide flanges. If twisting is neglected, the only modification of the procedure would be in the determination of the constant-curvature, moment-curvature curves. If twisting is considered, additional modification to the whole procedure would be necessary.

It would also be of interest to study the biaxially loaded column as an integral part of a braced frame. Experimental results are available for this type of study (1).

Case	Table 2.1 Equations for λ/P_y for Different Yield Configurations*
(a)	$[2\Phi^x - (\bar{\epsilon}_1 - \bar{\epsilon}_3 - 2)]\epsilon_o - 2P\Phi^y$
(b)	$-\epsilon_o^3 + [6K\Phi^y - 3(\bar{\epsilon}_2 - 1)]\epsilon_o^2 + [6K\Phi^y(\bar{\epsilon}_3 + \bar{\epsilon}_4 + 2) - 3(\bar{\epsilon}_2 - 1)^2 + 24K\Phi^x\Phi^y]\epsilon_o + [6K\Phi^y(\bar{\epsilon}_3 + 1)(\bar{\epsilon}_4 + 1) + 2K\Phi^y(\bar{\epsilon}_4 - \bar{\epsilon}_3)^2 - (\bar{\epsilon}_2 - 1)^3 - 24K\Phi^x\Phi^yP]$
(c)	$[2\Phi^x + 4K\Phi^y - \bar{\epsilon}_4 + 3 - 3(\bar{\epsilon}_2 - 1)]\epsilon_o^2 + [-2(2\Phi^x + \bar{\epsilon}_4 + 1)(K\Phi^y - \bar{\epsilon}_1 - 1) + 2K\Phi^y(2\bar{\epsilon}_3 + 5\bar{\epsilon}_4 + 5 + 12\Phi^x) + (\bar{\epsilon}_1 + 1)^2 - 3(\bar{\epsilon}_2 - 1)^2]\epsilon_o + [6K\Phi^y(\bar{\epsilon}_4 + 1)(\bar{\epsilon}_3 + 1) - (2\Phi^x + \bar{\epsilon}_4 + 1)(2K\Phi^y(\bar{\epsilon}_3 - 2\bar{\epsilon}_4 + 1) - (\bar{\epsilon}_1 + 1)^2) - 24K\Phi^x\Phi^yP - (\bar{\epsilon}_2 - 1)^3]$
(d)	$3\epsilon_o^2 + [3(\bar{\epsilon}_3 + \bar{\epsilon}_4 + 2) + 12\Phi^x]\epsilon_o + [3(\bar{\epsilon}_3 + 1)(\bar{\epsilon}_4 + 1) + (\bar{\epsilon}_4 - \bar{\epsilon}_3)^2 - 12\Phi^xP]$
(e)	$\epsilon_o^3 + [2\Phi^x + 4K\Phi^y - \bar{\epsilon}_4 + 3]\epsilon_o^2 + [-2(2\Phi^x + \bar{\epsilon}_4 + 1)(K\Phi^y - \bar{\epsilon}_1 - 1) + 2K\Phi^y(2\bar{\epsilon}_3 + 5\bar{\epsilon}_4 + 5 + 12\Phi^x) + (\bar{\epsilon}_1 + 1)^2]\epsilon_o + [6K\Phi^y(\bar{\epsilon}_4 + 1)(\bar{\epsilon}_3 + 1) - (2\Phi^x + \bar{\epsilon}_4 + 1)(2K\Phi^y(\bar{\epsilon}_3 - 2\bar{\epsilon}_4 + 1) - (\bar{\epsilon}_1 + 1)^2) - 24K\Phi^x\Phi^yP]$
(f)	$[2K\Phi^y - (\bar{\epsilon}_4 + \bar{\epsilon}_2 - 2)]\epsilon_o - 2K\Phi^yP$
(g)	$-\epsilon_o^3 + [6\Phi^x - 3(\bar{\epsilon}_2 - 1)]\epsilon_o^2 + [6\Phi^x(\bar{\epsilon}_3 + \bar{\epsilon}_1 + 2) - 3(\bar{\epsilon}_2 - 1)^2 + 24K\Phi^x\Phi^y]\epsilon_o + [6\Phi^x(\bar{\epsilon}_3 - 1)(\bar{\epsilon}_1 - 1) + 2\Phi^x(\bar{\epsilon}_1 - \bar{\epsilon}_3)^2 - (\bar{\epsilon}_2 - 1)^3 - 24K\Phi^x\Phi^yP]$
(h)	$3\epsilon_o^2 + [3(\bar{\epsilon}_3 + \bar{\epsilon}_1 + 2) + 12K\Phi^y]\epsilon_o + [3(\bar{\epsilon}_3 + 1)(\bar{\epsilon}_1 + 1) + (\bar{\epsilon}_1 - \bar{\epsilon}_3)^2 - 12K\Phi^yP]$
(i)	$-\epsilon_o^3 + [12K\Phi^x\Phi^y - 3(\bar{\epsilon}_3 + 1)^2]\epsilon_o + -[12K\Phi^x\Phi^yP]$
(j)	$-\epsilon_o^3 + [-3(\bar{\epsilon}_3 + 1)]\epsilon_o^2 + [24K\Phi^x\Phi^y - 3(\bar{\epsilon}_3 + 1)^2]\epsilon_o + [-24K\Phi^x\Phi^yP - (\bar{\epsilon}_3 + 1)^3]$

* All strains are in terms of ϵ_y, curvatures are in terms of Φ^x_y and the load in P_y

Case	Table 2.2 Equations for M^x/M^x_y for Different Yield Configurations*
(a)	$\left[8(\phi^x)^3 + (\bar{\epsilon}_1 - 1)(\bar{\epsilon}_2 - 1)(\bar{\epsilon}_1 + \bar{\epsilon}_2 - 2 - 4\phi^x) + \epsilon_o^2(\bar{\epsilon}_1 + \bar{\epsilon}_2 - 2 - 2\phi^x) + (\bar{\epsilon}_1 - 1)^2(\bar{\epsilon}_1 - 1 - 4\phi^x) + (\bar{\epsilon}_2 - 1)^2(\bar{\epsilon}_2 - 1 - 4\phi^x)\right] / 8(\phi^x)^2$
(b)	$\phi^x\left[1 + 5a_{31}^3 - a_{31}^2 + \frac{1}{2}(a_{31}^2 a_{42}) - a_{31}a_{42} + \frac{1}{2}(a_{31}a_{42}^2) - a_{42}^2 + \frac{1}{2}(a_{42})^3 - a_{21}a_{24}^2 + \frac{1}{2}(a_{21}a_{24}^3)\right]$
(c)	$\frac{1}{2}\,\phi^x\left[(1 - a_{12})(1 + a_{42})(1 - a_{42})^2 - a_{24}^2 a_{21}\,(2 - a_{24})\right]$
(d)	$\phi^x\left[1 + 5a_{31}^3 - a_{31}^2 + \frac{1}{2}(a_{31}^2 a_{42}) - a_{31}a_{42} + \frac{1}{2}(a_{31}a_{42}^2) - a_{42}^2 + \frac{1}{2}(a_{42})^3\right]$
(e)	$\frac{1}{2}\,\phi^x\,(1 - a_{12})(1 - a_{42})^2(1 + a_{42})$
(f)	$\left[(2K\phi^y + \bar{\epsilon}_1 - \bar{\epsilon}_2 + 2)\,\phi^x\right] / (2K\phi^y)$
(g)	$\frac{1}{2}\,\phi^x\left[2 - a_{12} - a_{34} - a_{21}a_{24}^2(2 - a_{24})\right]$
(h)	$\frac{1}{2}\,\phi^x\left[2 - a_{12} - a_{34}\right]$
(i)	$\frac{1}{2}\,\phi^x\left[2 - a_{31}^2 a_{34}(2 - a_{31}) - a_{21}a_{24}^2(2 - a_{24})\right]$
(j)	$\frac{1}{2}\,\phi^x\left[2 - a_{31}^2 a_{34}(2 - a_{31})\right]$

*All strains are in terms of ϵ_y and all curvatures are in terms of ϕ^x_y.

Case	Table 2.3 Equations for M^y/M^x_y for Different Yield Configurations*
(a)	$\left[(2\Phi^x + 2 - \bar{\epsilon}_1 - \bar{\epsilon}_2)K^2\Phi^y\right] / (2\Phi^x)$
(b)	$\frac{1}{2}K^2\Phi^y\left[2 - a_{42} - a_{31} - a_{21}a_{24}{}^2 (2 - a_{21})\right]$
(c)	$\frac{1}{2}K^2\Phi^y\left[(1 - a_{42})(1 + a_{12})(1 - a_{12})^2 - a_{21}{}^2a_{24} (2 - a_{21})\right]$
(d)	$\frac{1}{2}K^2\Phi^y (2 - a_{42} - a_{31})$
(e)	$\frac{1}{2}K^2\Phi^y (1 - a_{42})(1 - a_{12})^2(1 + a_{12})$
(f)	$\left[8(K\Phi^y)^3 - (\bar{\epsilon}_1 + 1)(\bar{\epsilon}_2 - 1)(\bar{\epsilon}_2 - \bar{\epsilon}_1 - 2 - 4K\Phi^y) + 6\epsilon_o^2(\bar{\epsilon}_2 - \bar{\epsilon}_1 - 2 - 2K\Phi^y) - (\bar{\epsilon}_1 + 1)^2(\bar{\epsilon}_1 + 1 + 4K\Phi^y) + (\bar{\epsilon}_2 - 1)^2(\bar{\epsilon}_2 - 1 - 4K\Phi^y)\right] / (8K(\Phi^y)^2)$
(g)	$K^2\Phi^y\left[1 + 5a_{34}{}^3 - a_{34}{}^2 + \frac{1}{2}(a_{34}{}^2a_{12}) - a_{34}a_{12} + \frac{1}{2}(a_{34}a_{12}{}^2) - a_{12}{}^2 + a_{12}{}^3 - \frac{1}{2}(a_{21}{}^2a_{24})(2 - a_{21})\right]$
(h)	$K^2\Phi^y\left[1 + 5a_{34}{}^3 - a_{34}{}^2 + \frac{1}{2}(a_{34}{}^2a_{12}) - a_{34}a_{12} + \frac{1}{2}(a_{34}a_{12}{}^2) - a_{12}{}^2 + a_{12}{}^3\right]$
(i)	$\frac{1}{2}K^2\Phi^y\left[2 - a_{34}{}^2a_{31}(2 - a_{34}) - a_{21}{}^2a_{24}(2 - a_{21})\right]$
(j)	$\frac{1}{2}K^2\Phi^y\left[2 - a_{34}{}^2a_{31}(2 - a_{34})\right]$

*All strains are in terms of ϵ_y and all curvatures are in terms of Φ^x_y.

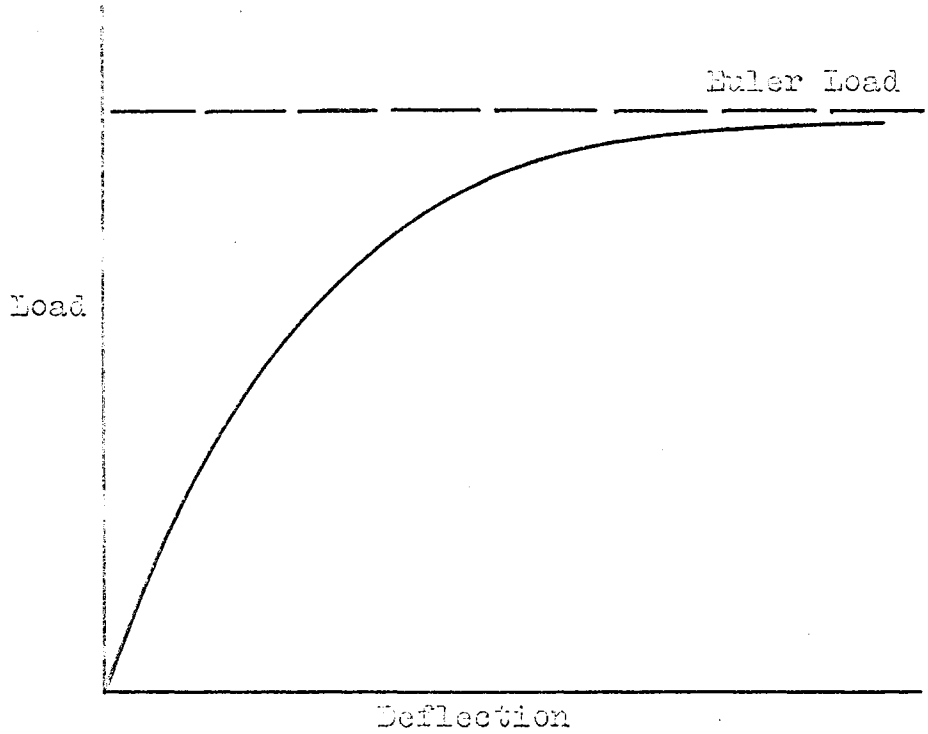

Fig. 1.1 Failure at the Euler Load

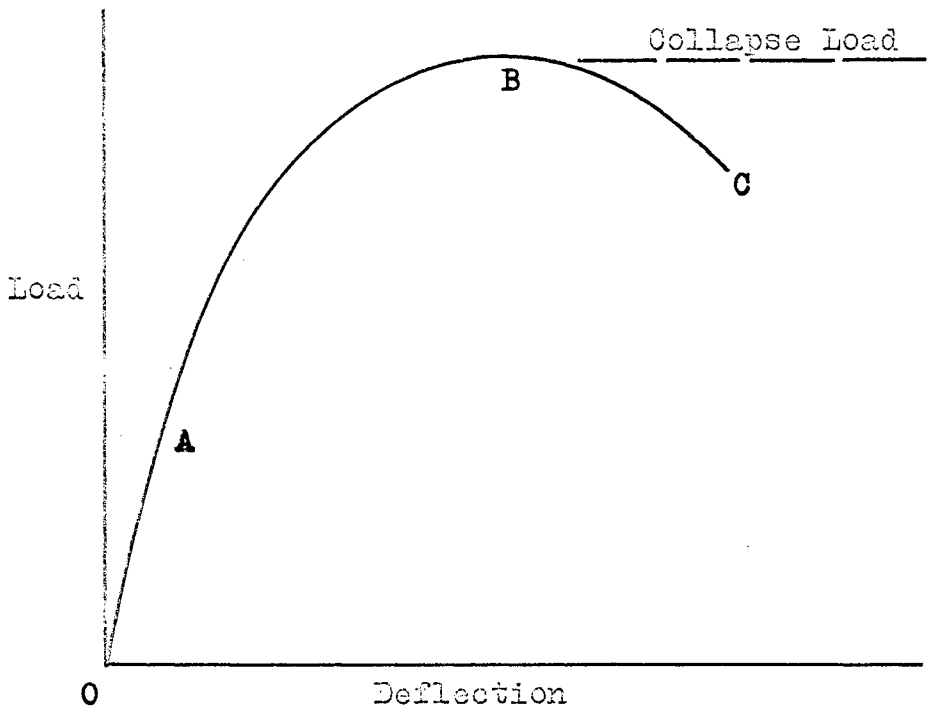

Fig. 1.2 Failure at the Collapse Load

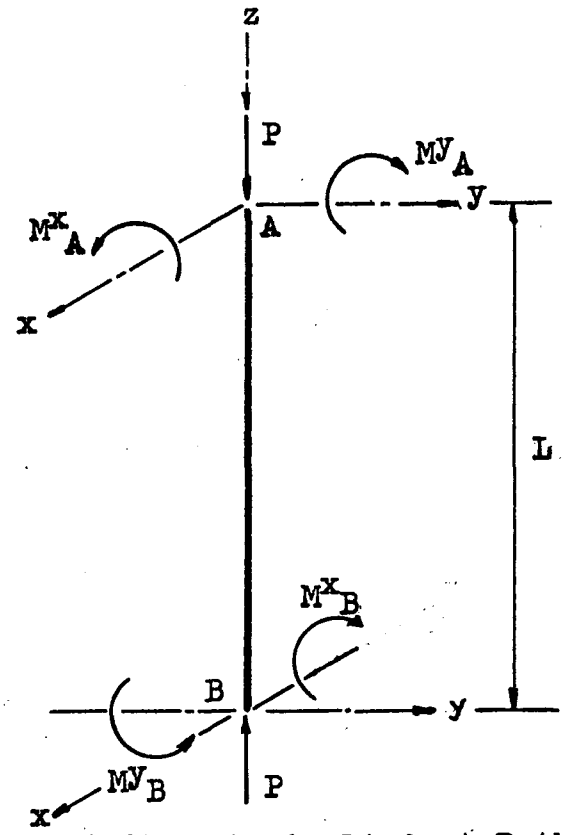

Fig. 2.1 Column with Moments Applied at Both Ends, $\beta = 1$

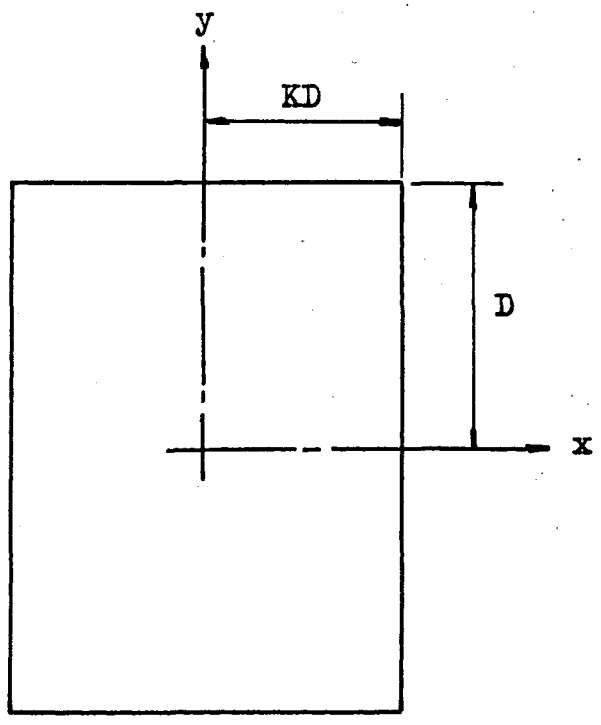

Fig. 2.2 Typical Solid Column Cross Section

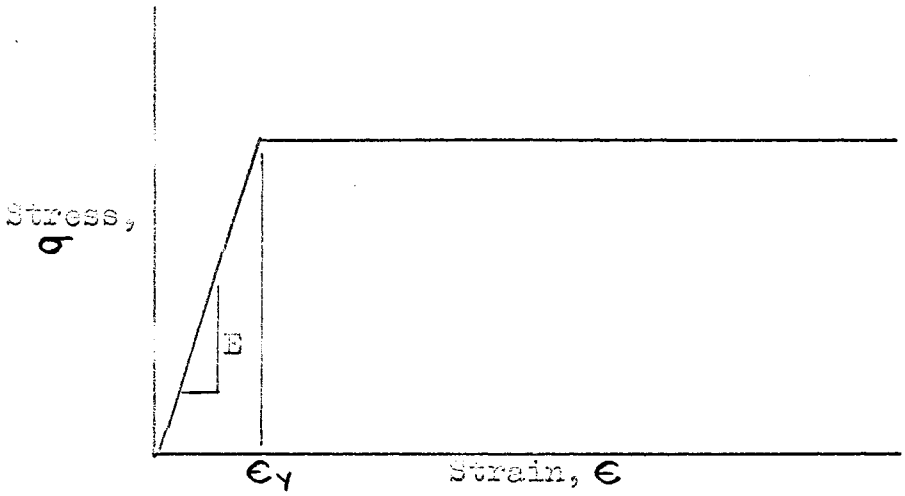

Fig. 2.3 Stress-Strain Curve for the Material

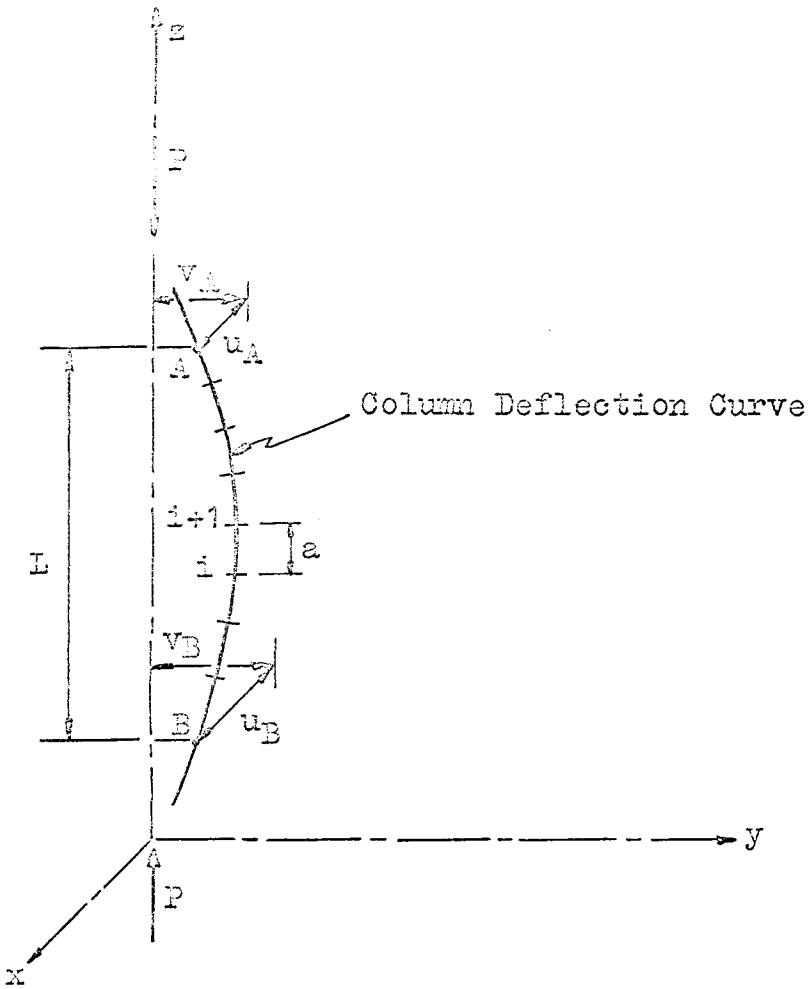

Fig. 2.4 Typical Column Deflection Curve

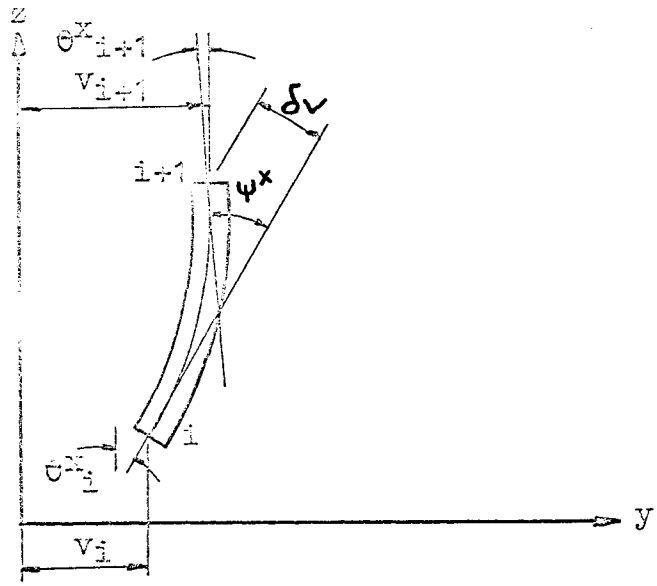

(a) Projection onto the y-z Plane

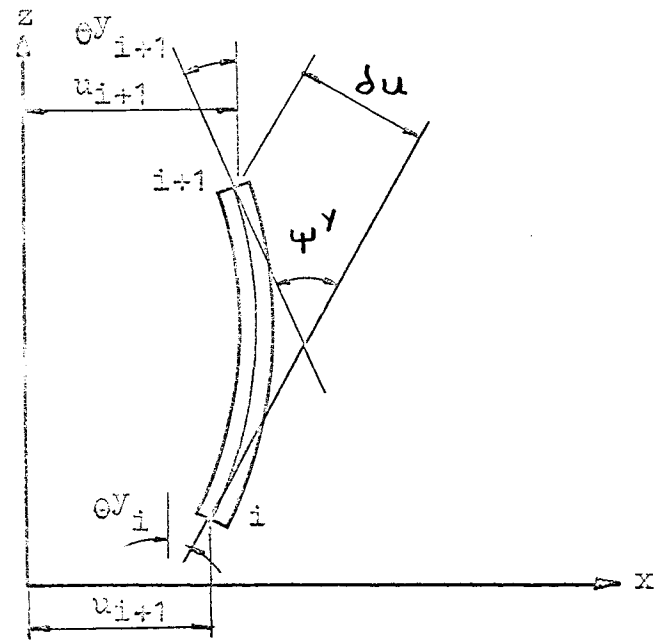

(b) Projection onto the x-z Plane

Fig. 2.5 Projections of the Column Element

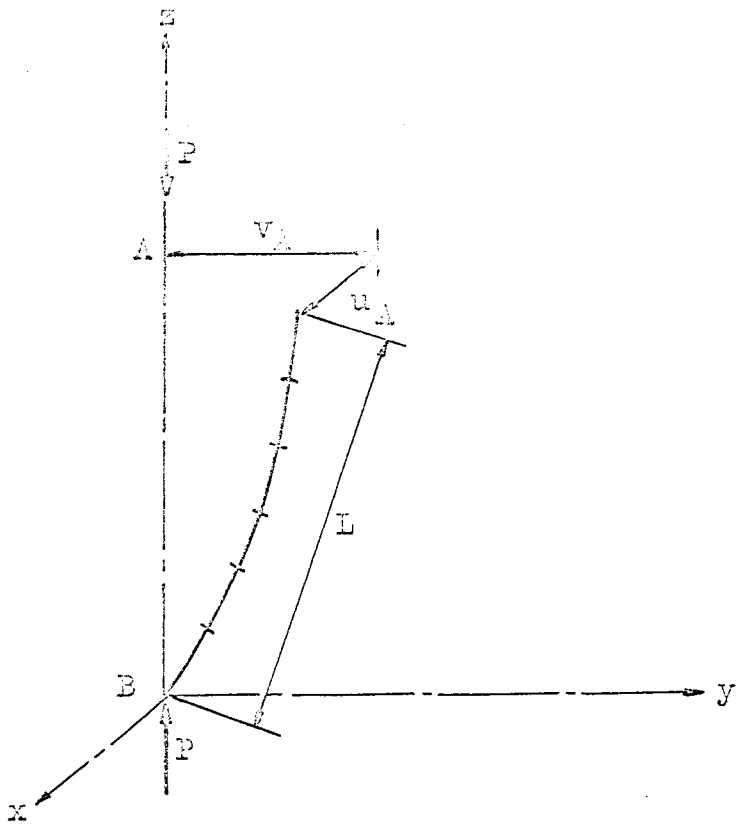

Fig. 2.6 Column Deflection Curve, $\beta = 0$

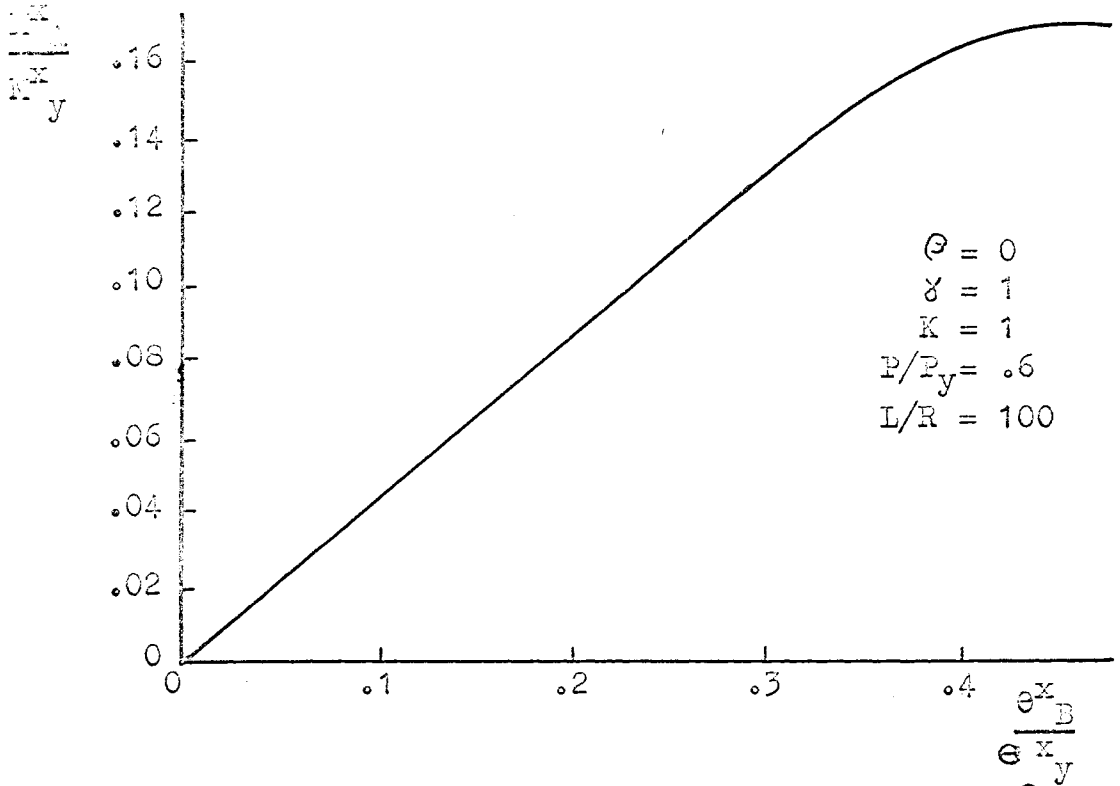

Fig. 2.7 Plot to Find the Maximum Moment, $\beta = 0$

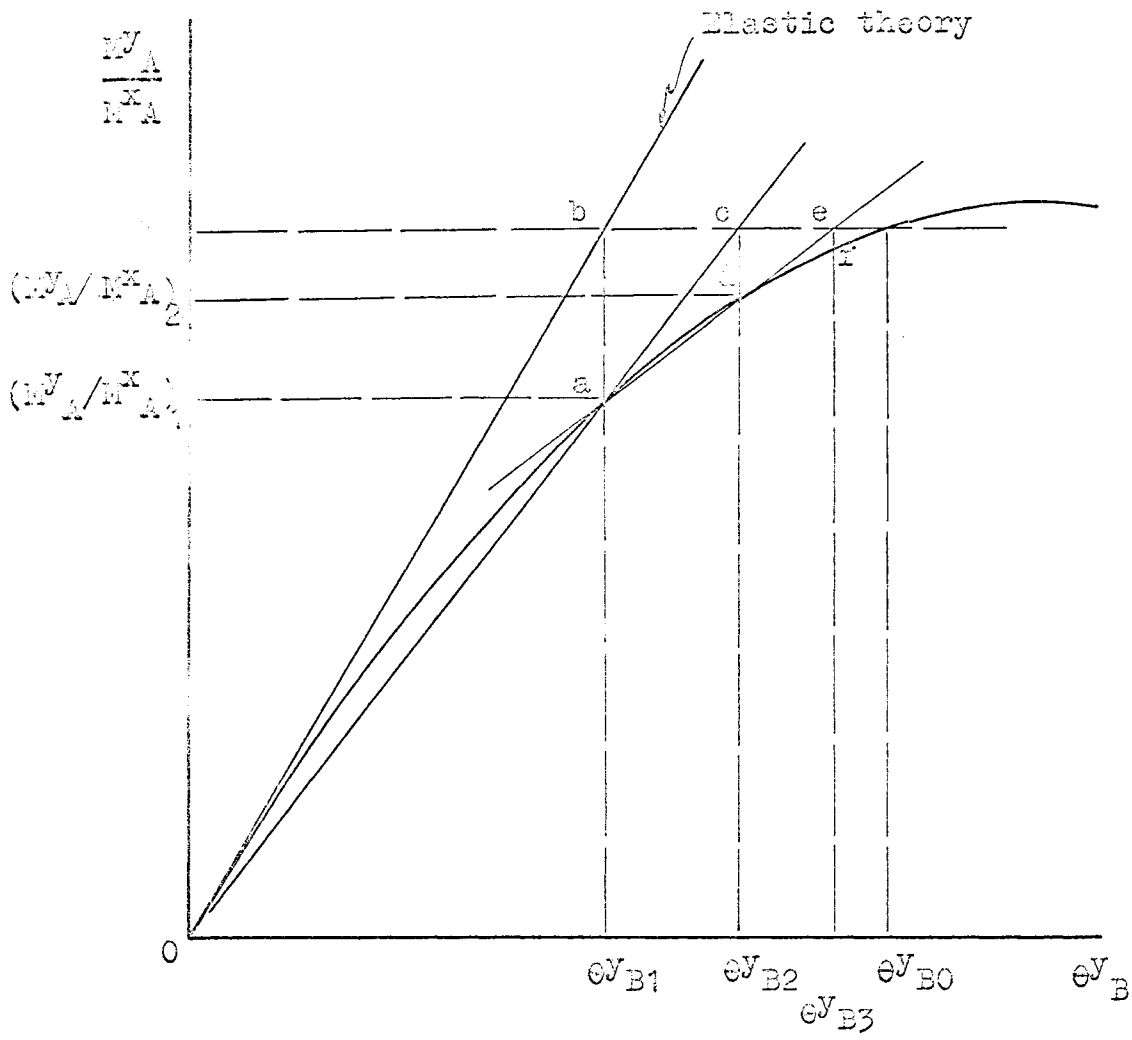

Fig. 2.3 Correction for θ^y_B

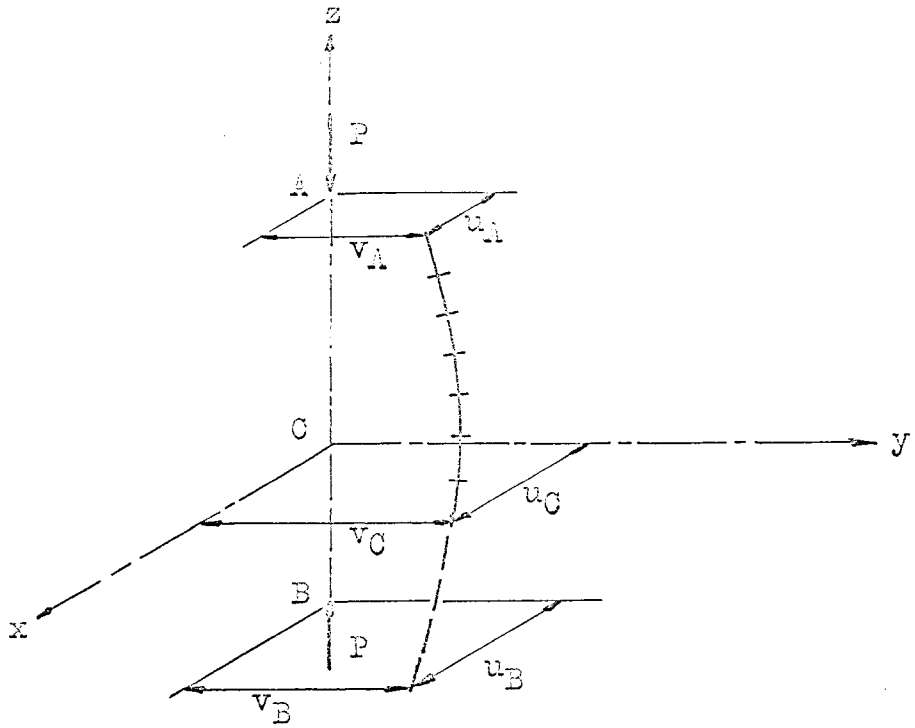

Fig. 2.9 Column Deflection Curve, $\rho = 1$

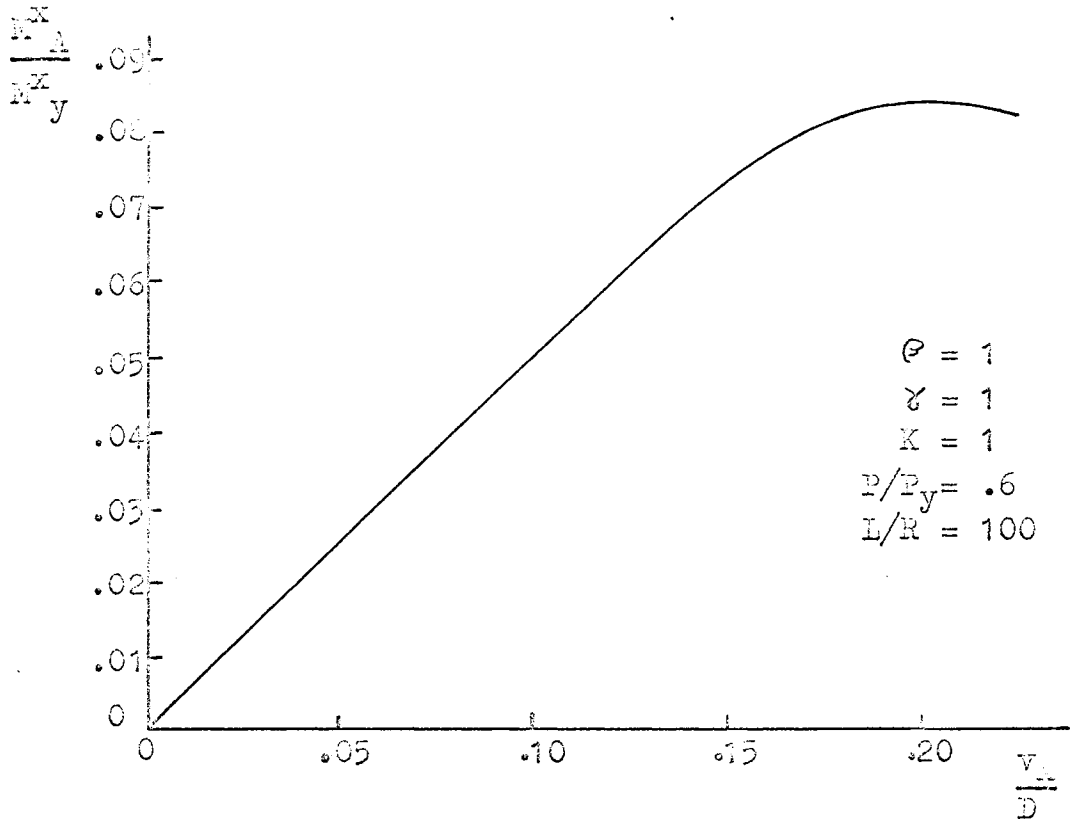

Fig. 2.10 Plot to Find the Maximum Moment, $\beta = 1$

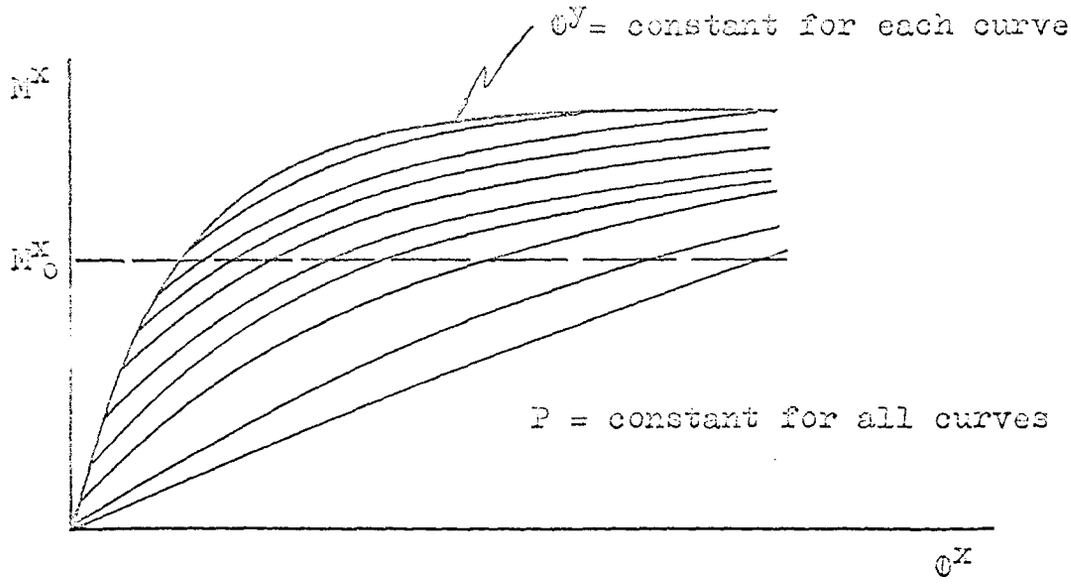

Fig. 2.11 Moment-Curvature Curves about the x-axis

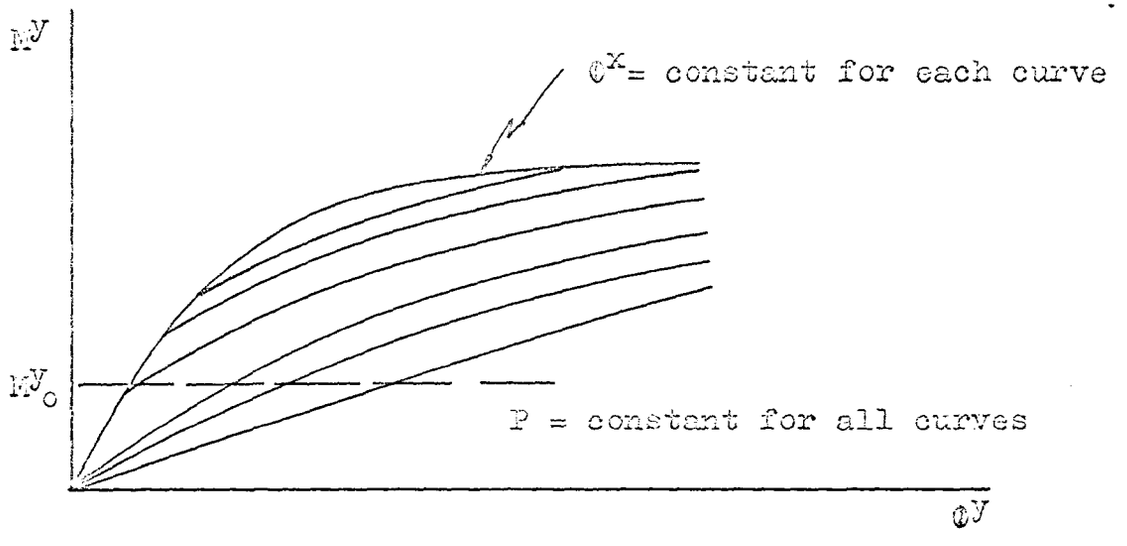

Fig. 2.12 Moment-Curvature Curves about the y-axis

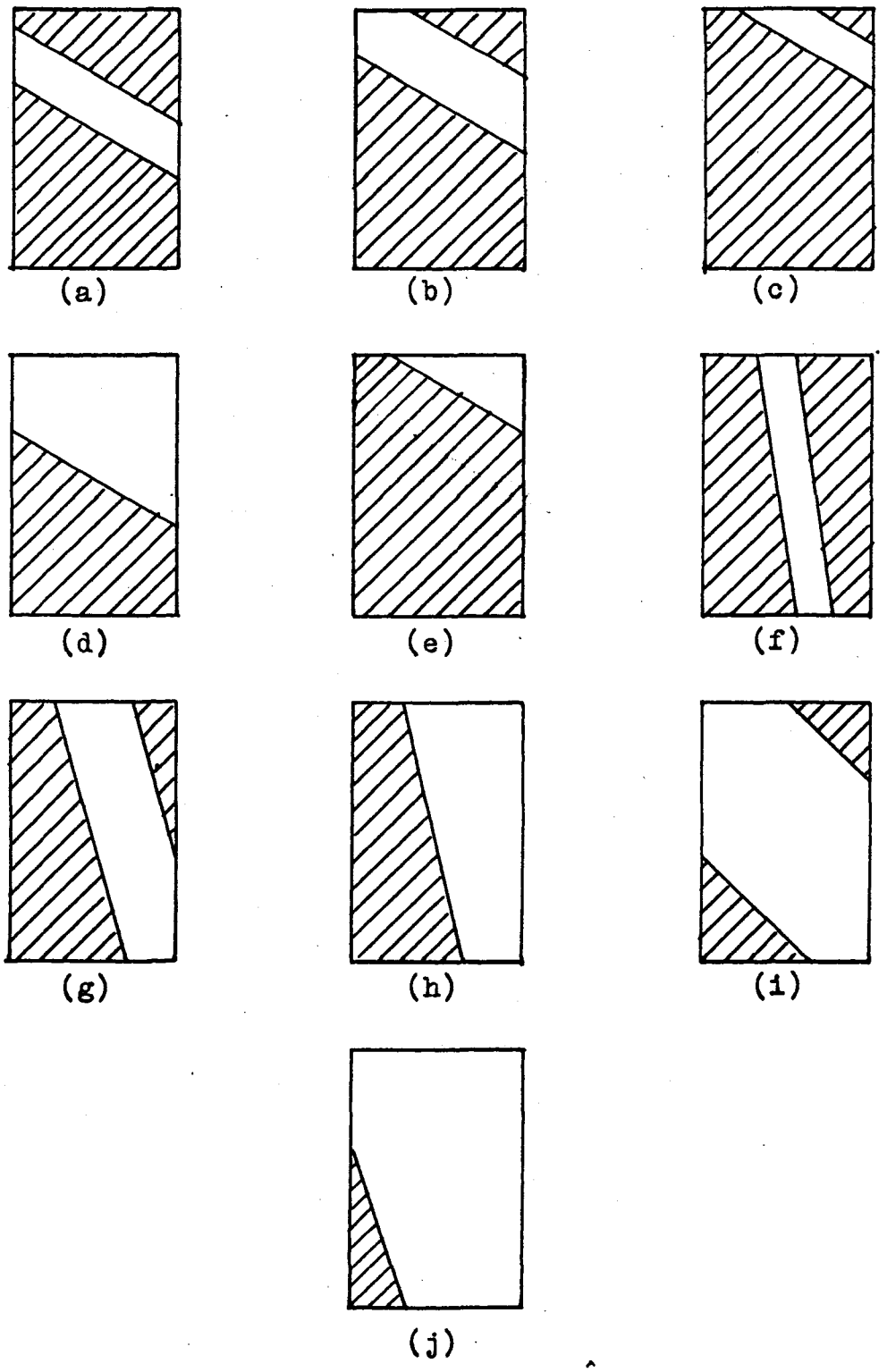

Fig. 2.13 Possible Yield Configurations for the Column Cross Section

(shaded portions represent yielded material)

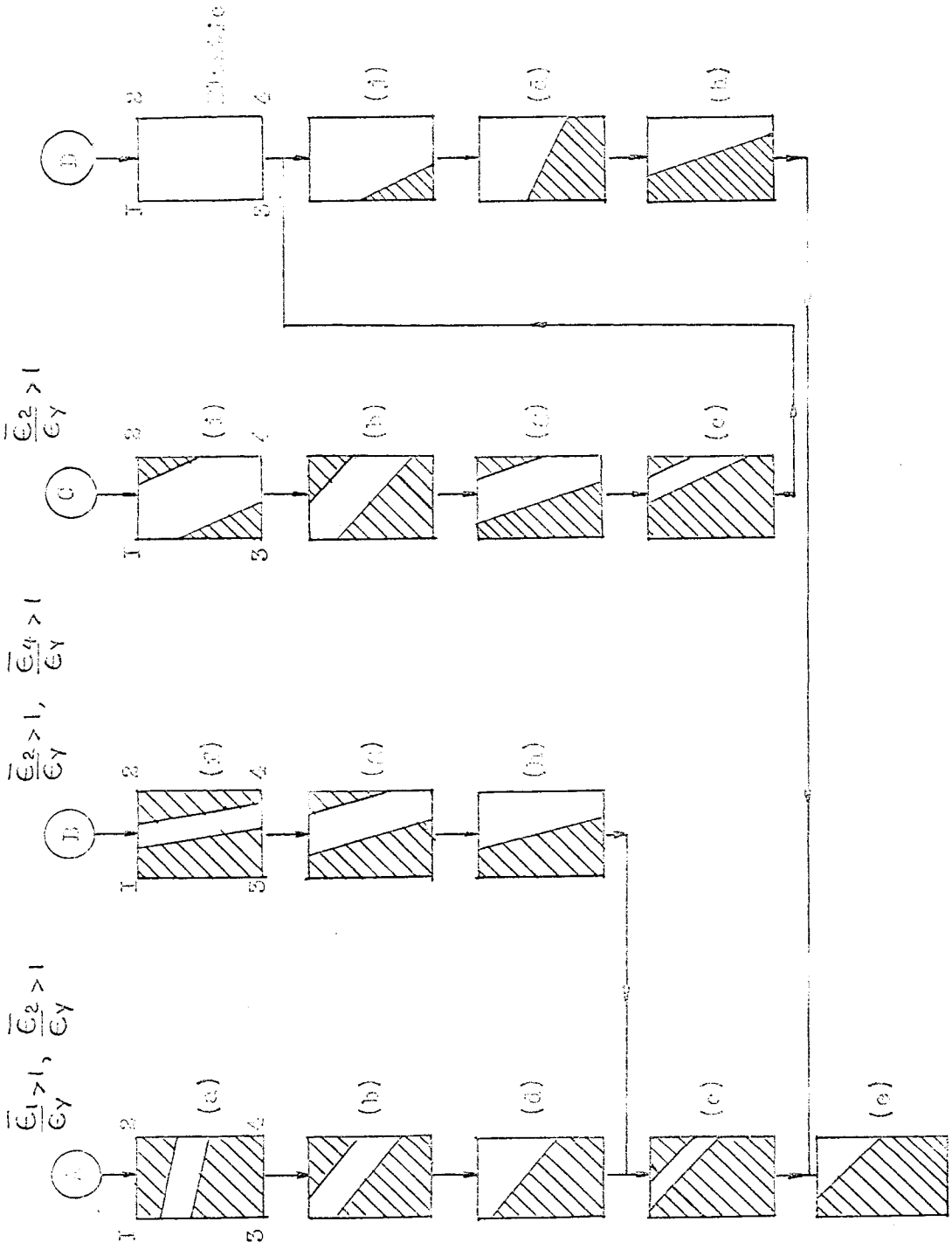

FIG. 2.14 SQUARED FOR CYCLIC HARDENING CONDITIONS

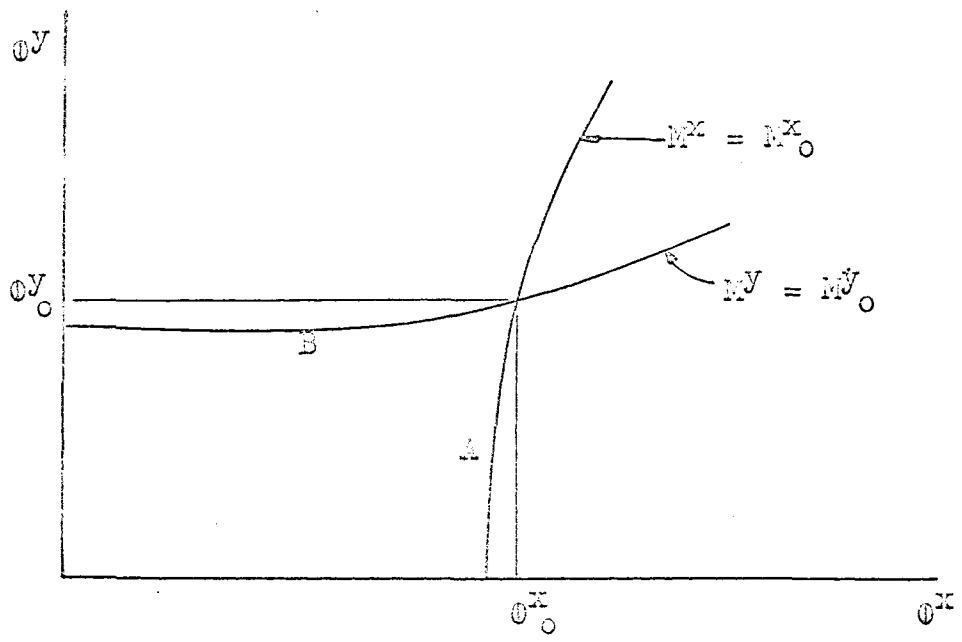

Fig. 2.15 Curvature Relationship for Constant Moment about each axis

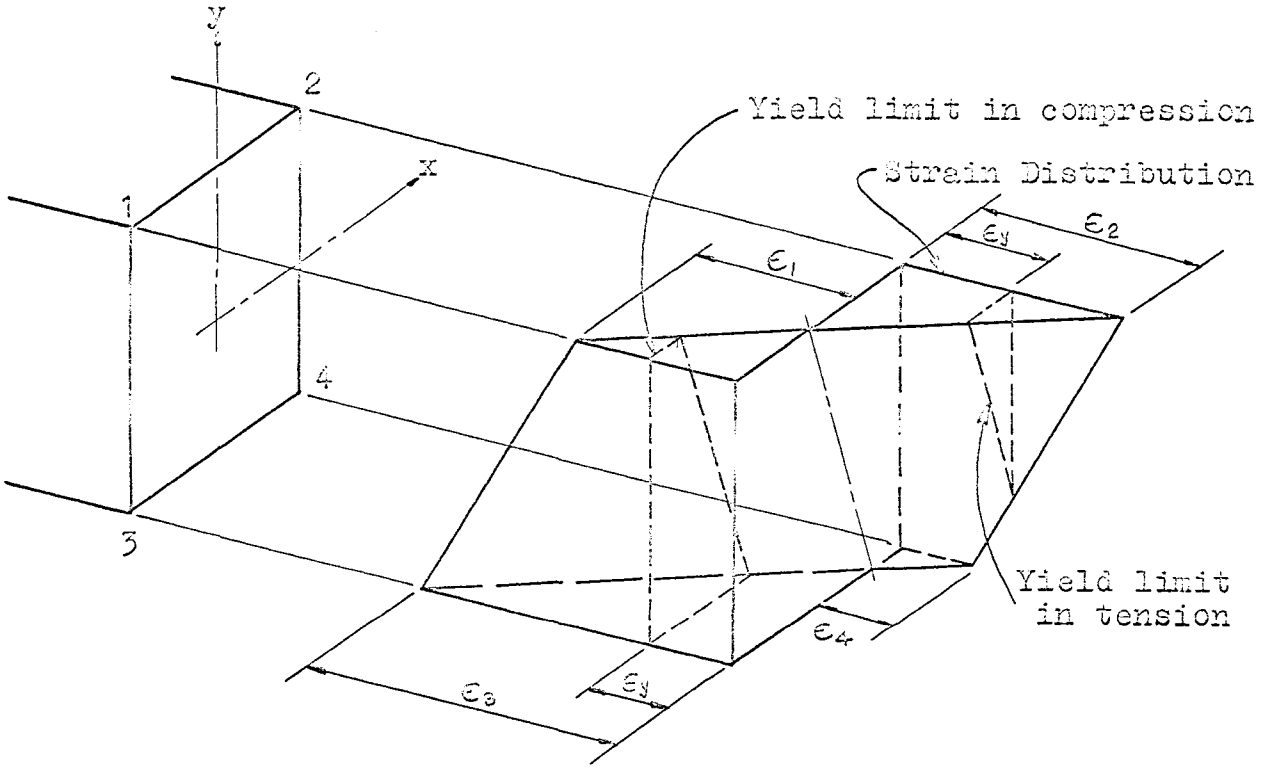

Fig. 2.16 Typical Strain Distribution on the Column Section

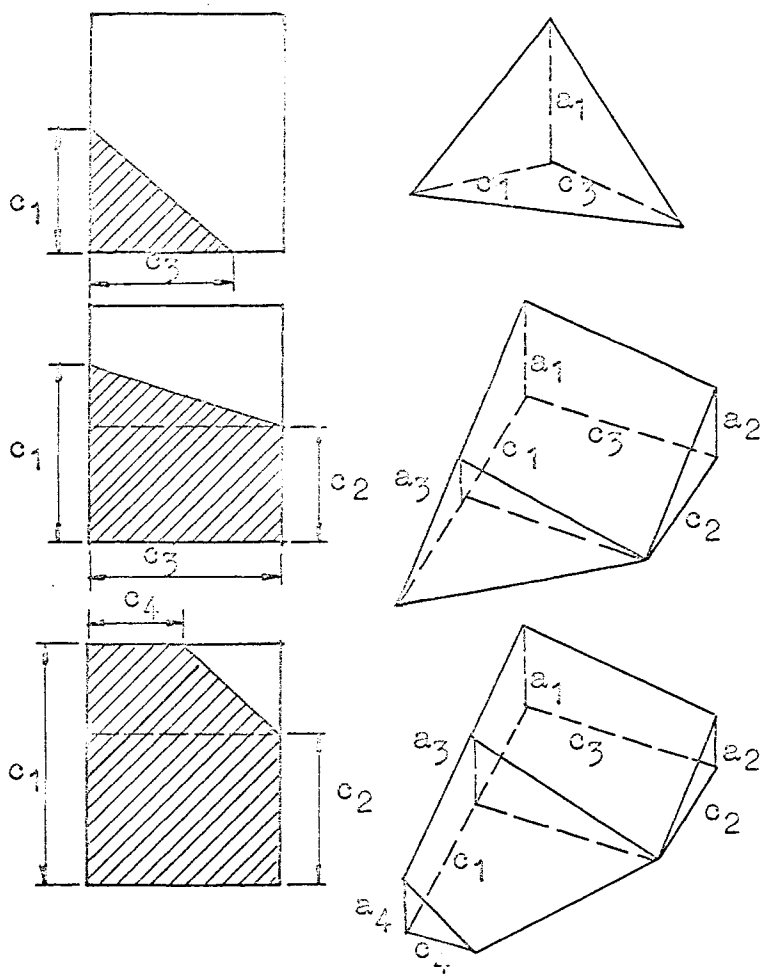

Fig. 2.17 Yield Volumes

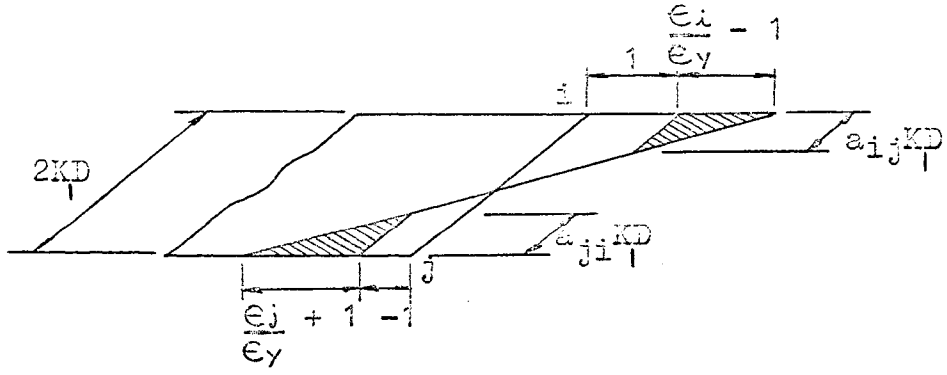

Fig. 2.18 Yield Configuration along an Edge

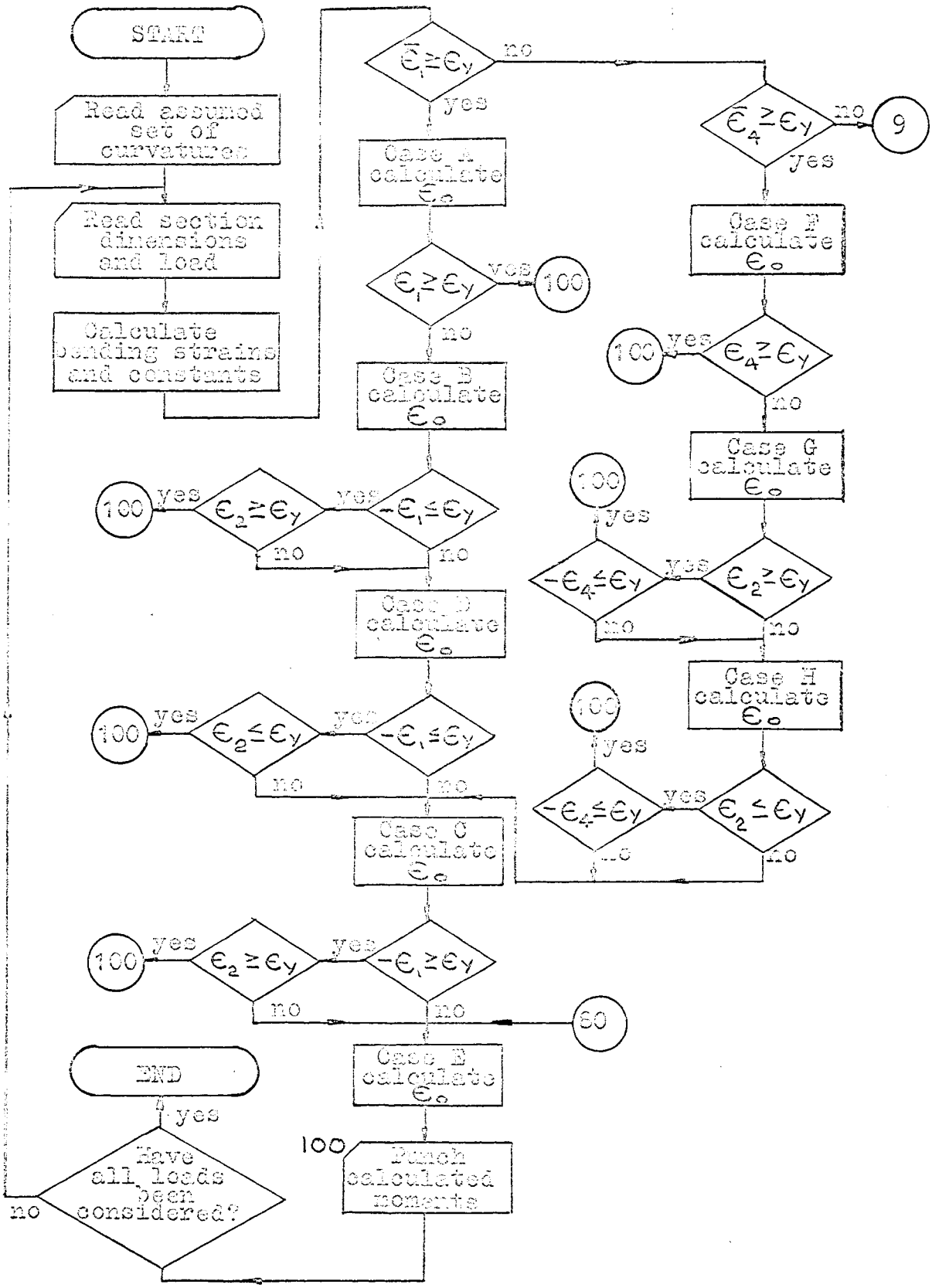

Fig. 3.1 Flow Diagram for Moment-Curvature Program

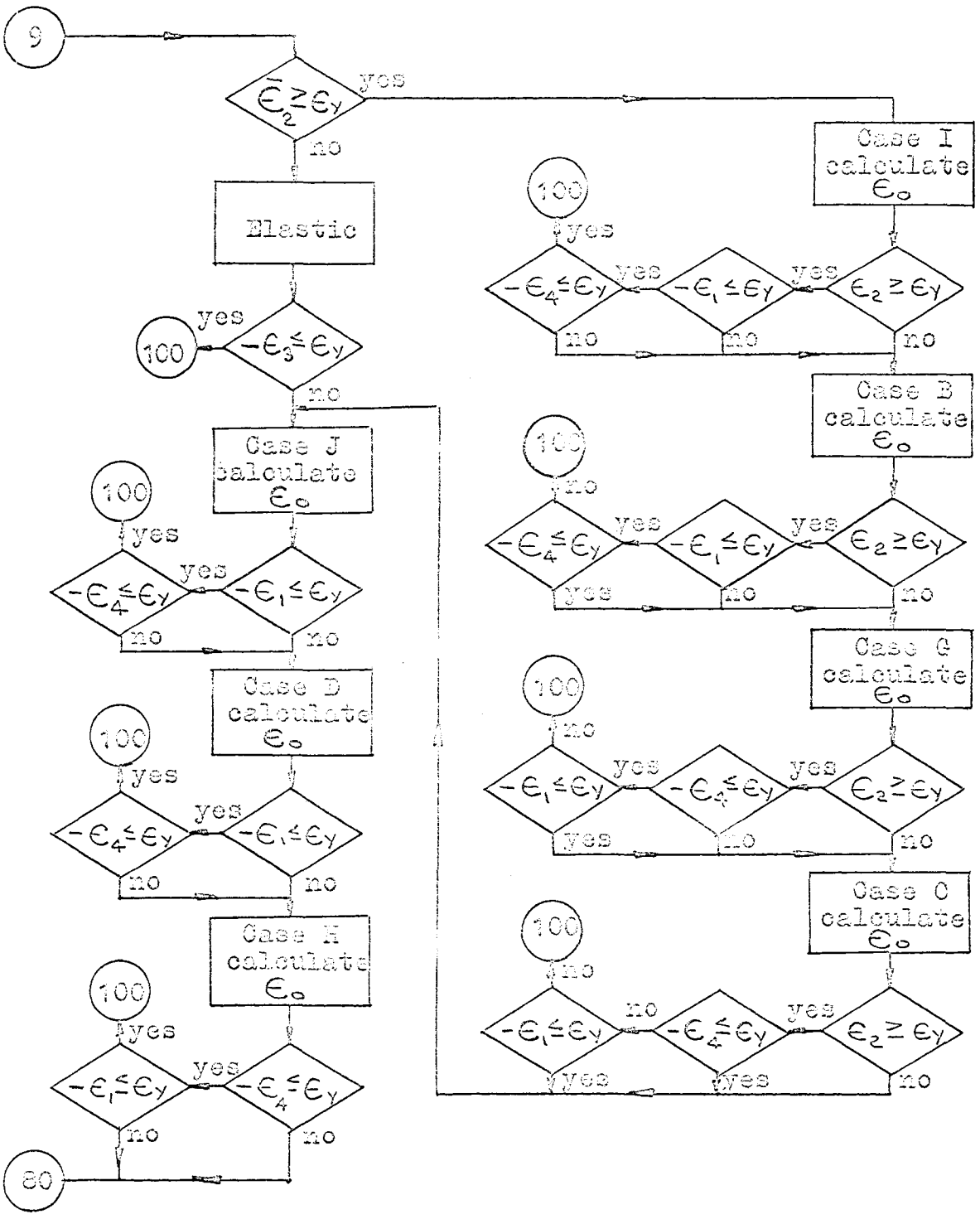

Fig. 3.1 (cont'd)

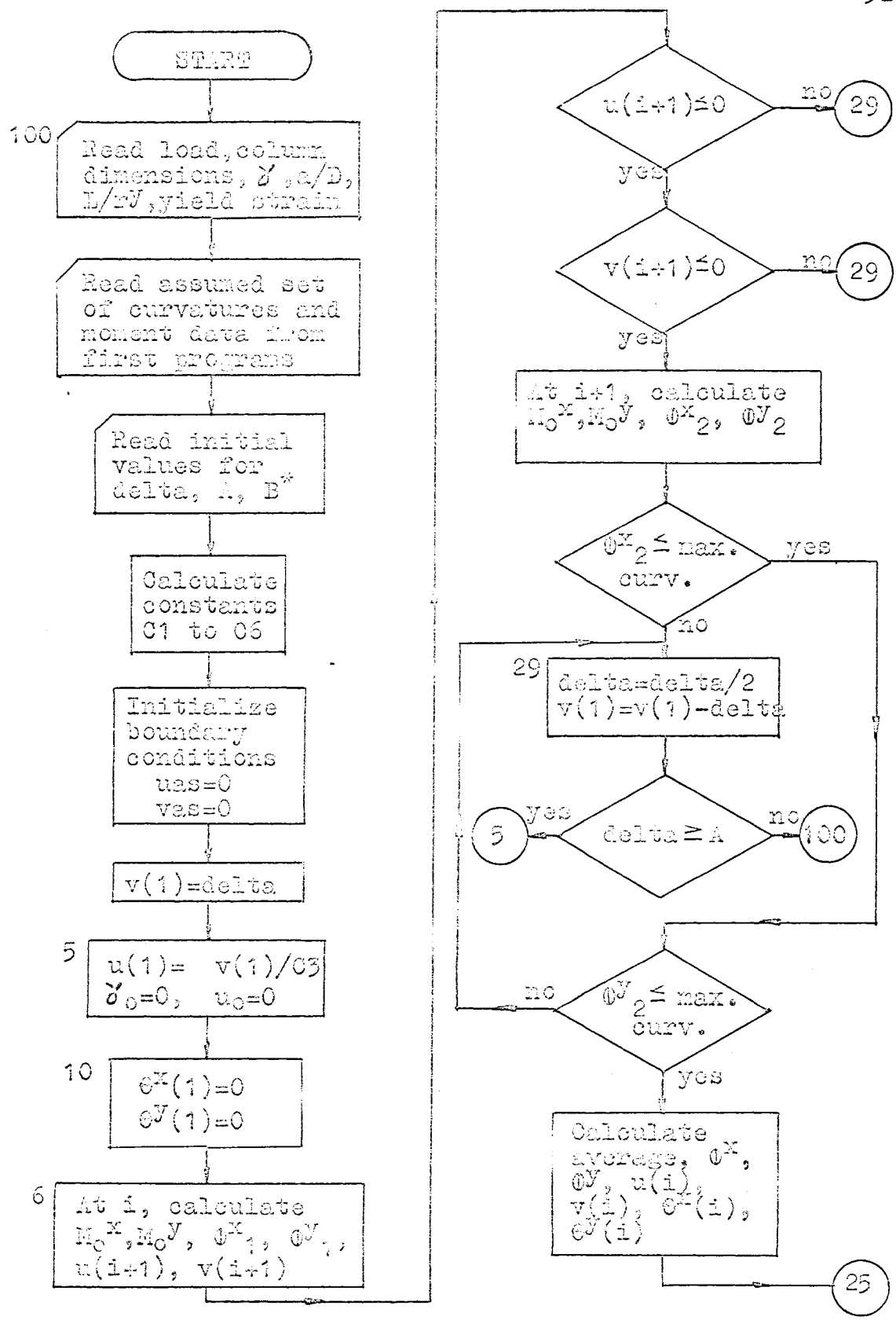

Fig. 3.2 Flow Diagram used to Determine Column Deflection Curves, $\epsilon = 1$

* Delta, A and B are defined in the list of notations.

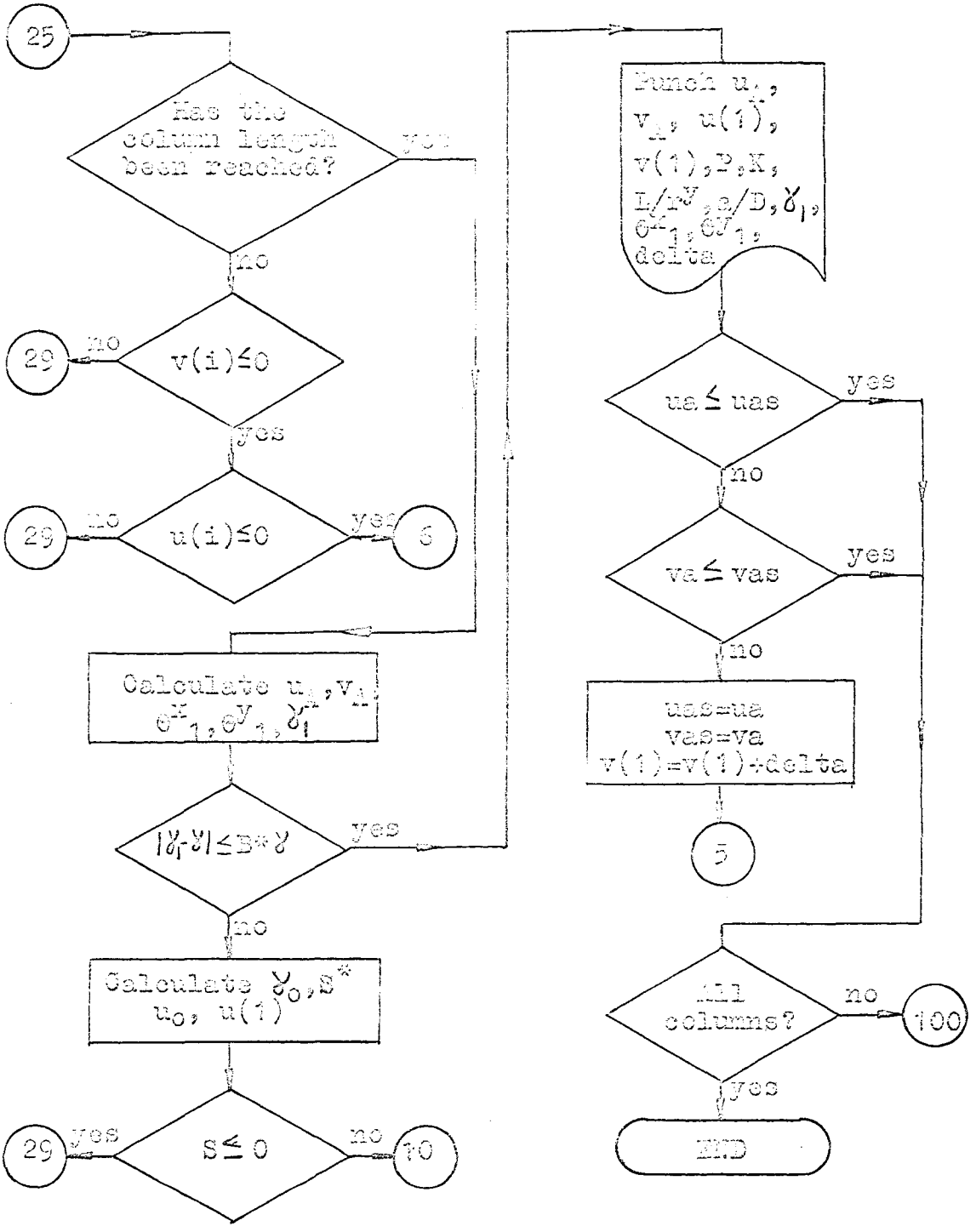

Fig. 3.2 (cont'd)

*S is defined in the list of notations.

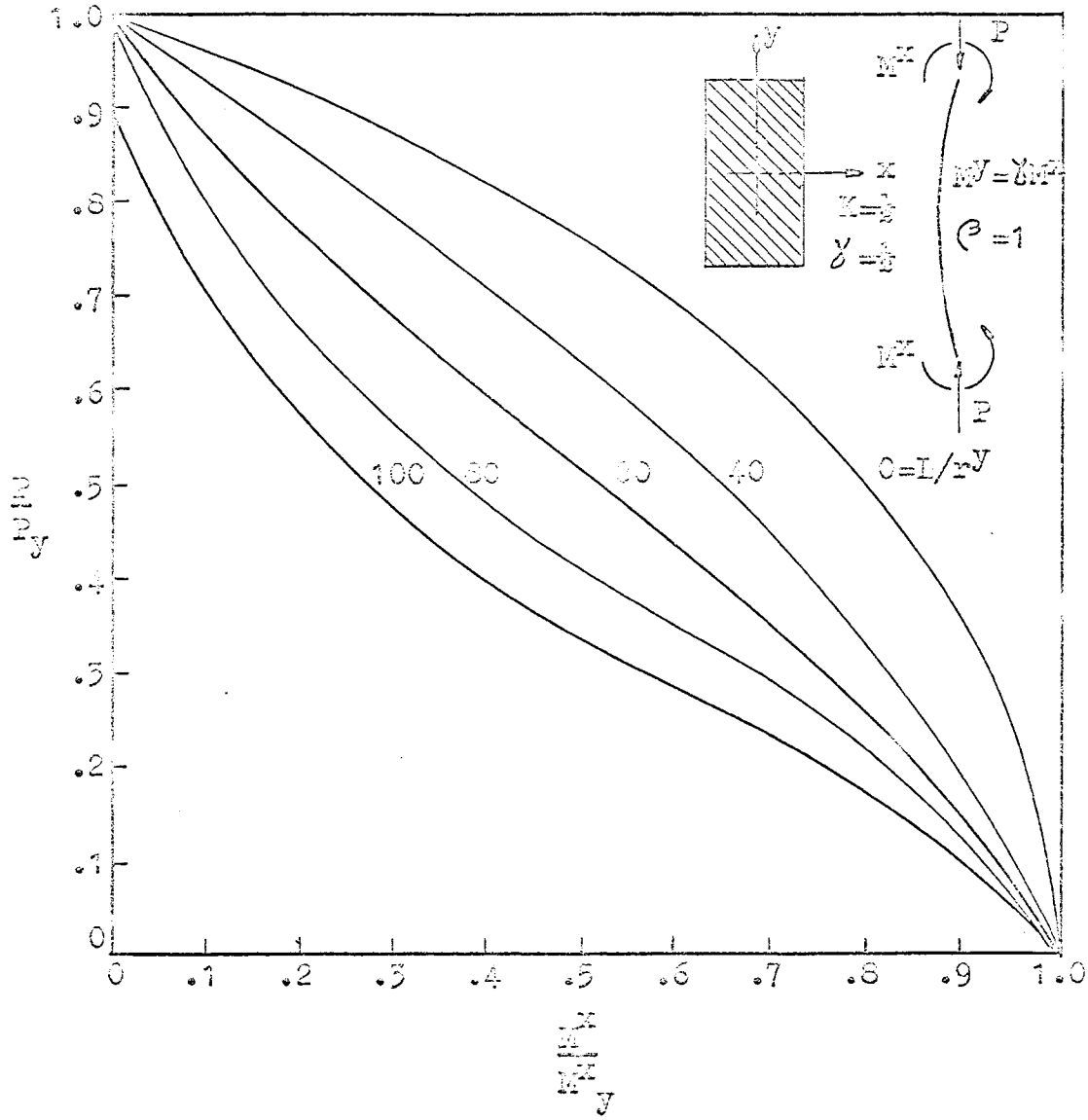

Fig. 4.1 Interaction Curves, $\beta = 1$

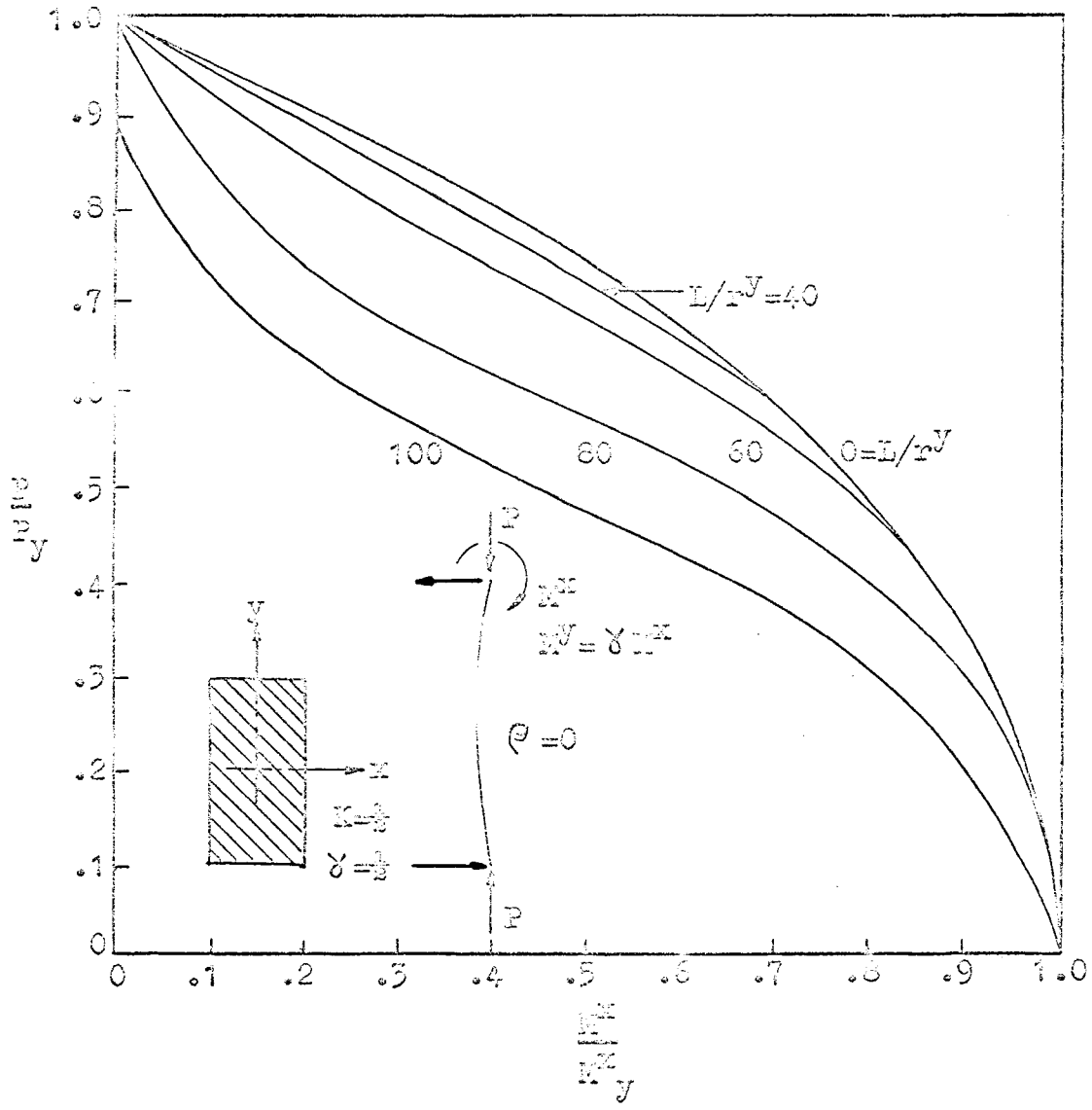

Fig. 4.2 Interaction Curves, $Q = 0$

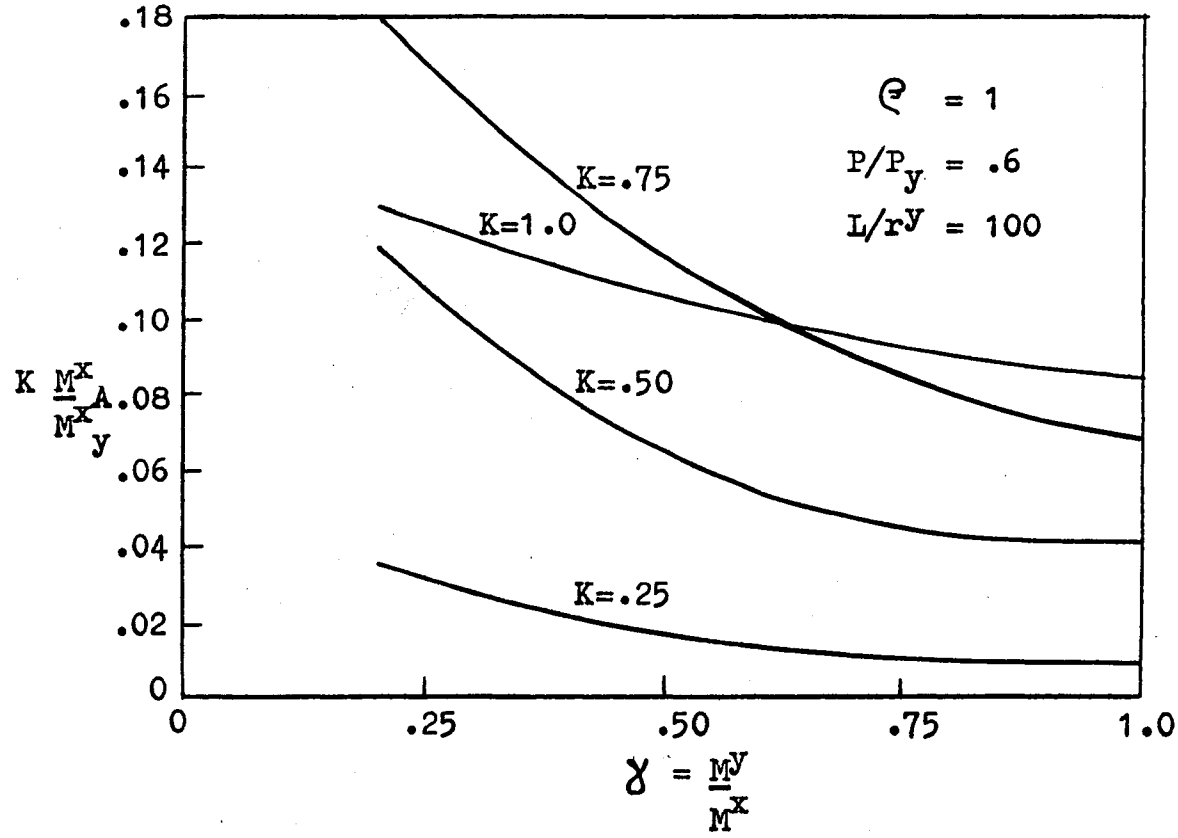

Fig. 4.3 Variation of End Moment with Moment Ratio, φ =1

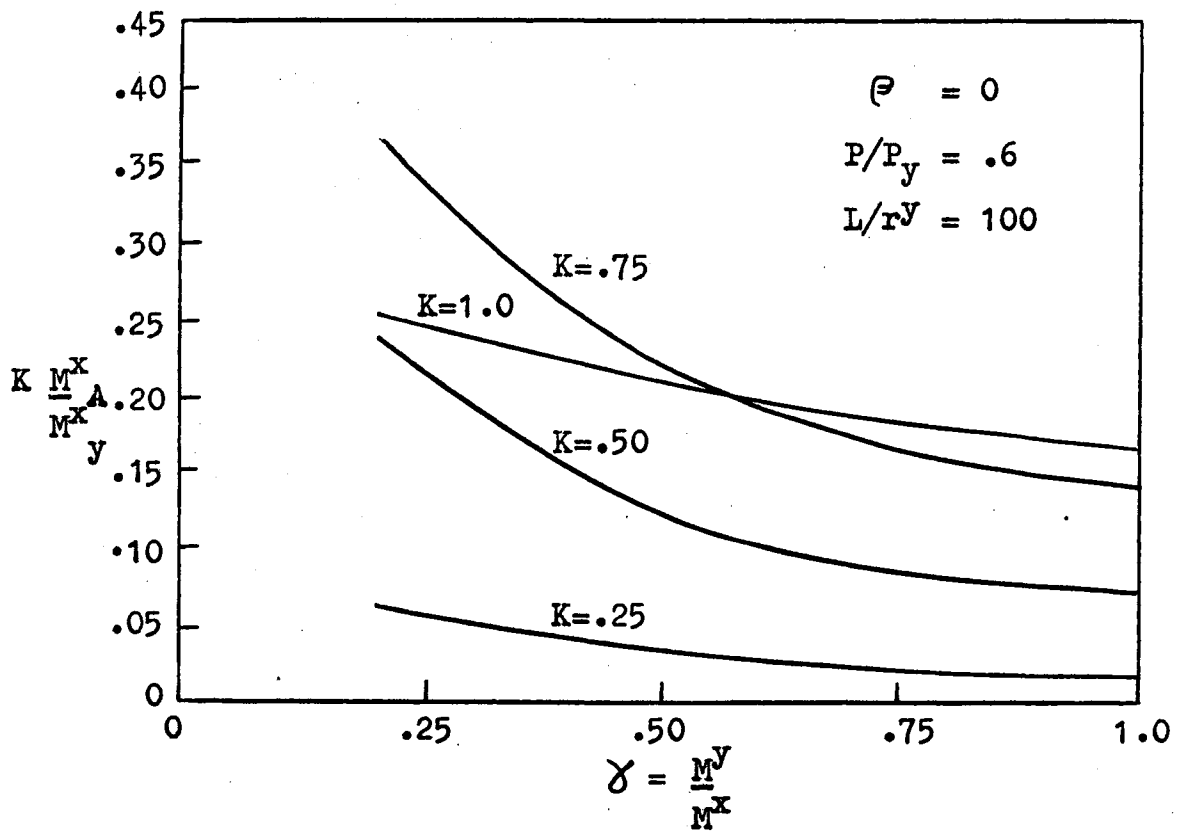

Fig. 4.4 Variation of End Moment with Moment Ratio, φ =0

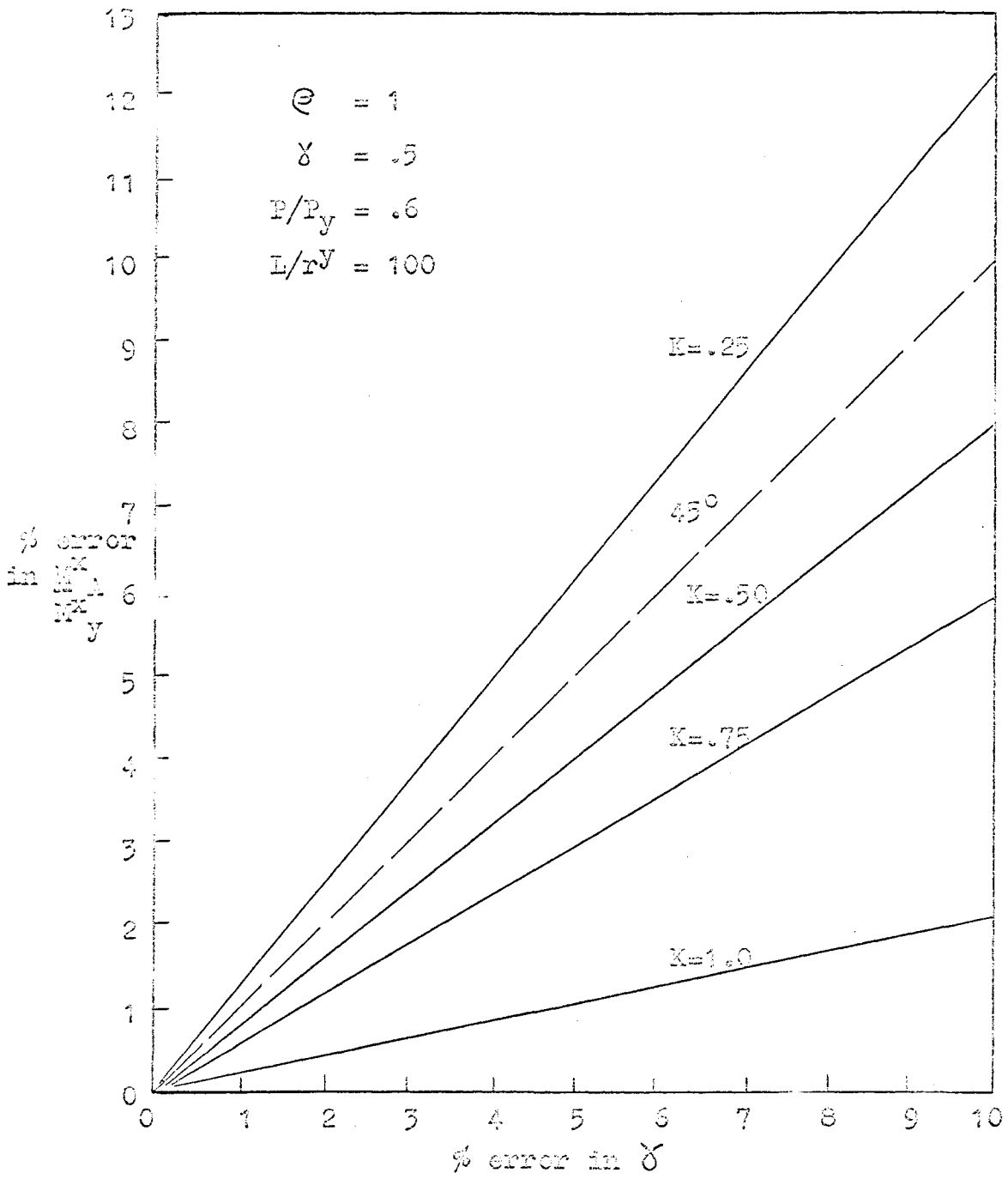

Fig. 4.5 Variation of Error in End Moment with Error in γ

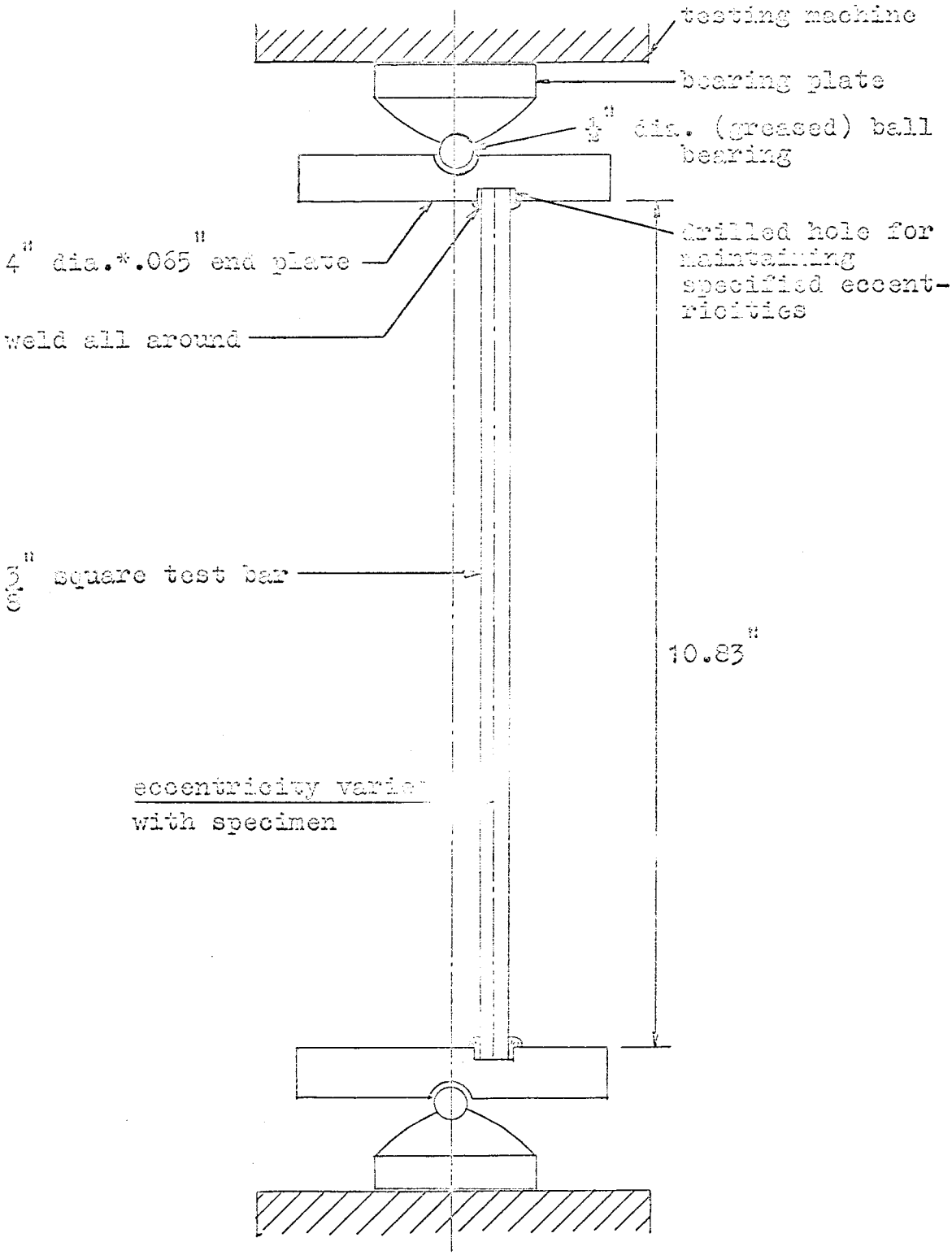

Fig. 4.6 Test Set-up

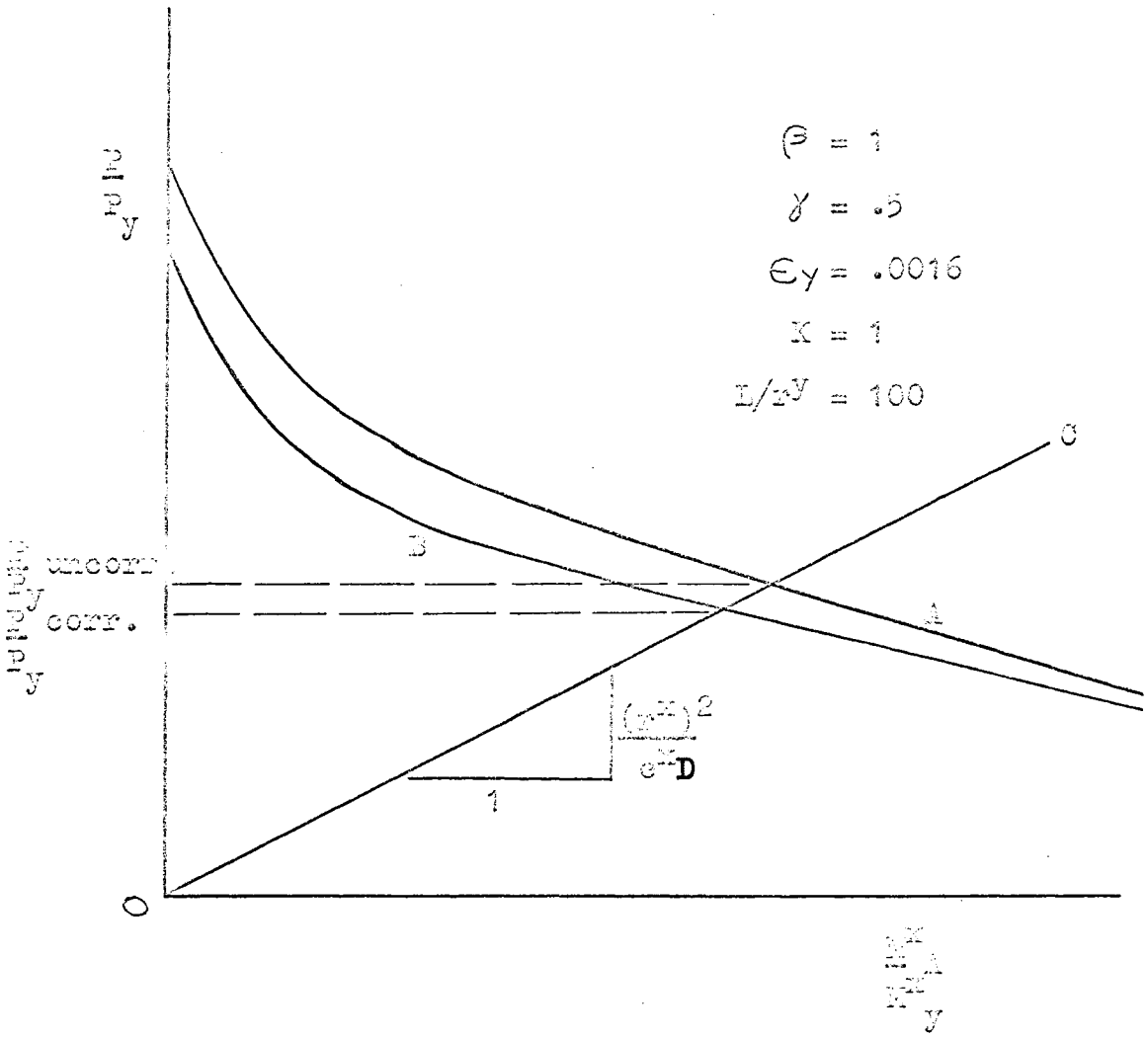

Fig. 4.7 Interaction Curve Showing Correction due to End Plates

BIBLIOGRAPHY

1. Baker, A. L. L., M. R. Horne and J. Heyman, The Steel Skeleton, Vol. 2, Plastic Behaviour and Design, Cambridge University Press, 1956.

2. Bijlaard, P. P., Buckling of Columns with Equal and Unequal Eccentricities and on Partial Rotational and Restraints, Proceedings, 2nd U.S. Nat'l Congress of Applied Mech., 1954.

3. Birnstiel, C., and J. Michalos, Ultimate Load of H-Columns Under Biaxial Bending, Proceedings, ASCE, Vol. 89, ST2, 1963.

4. Bleich, F., Buckling Strength of Metal Structures, McGraw-Hill Book Co., New York, 1952.

5. Commentary on Plastic Design in Steel, ASCE Manual of Engineering Practice No. 41, 1961.

6. Ellis, J. S., Plastic Behaviour of Compression Members, EIC, Vol. 2, No. 2, 1958.

7. Ellis, J. S., D. J. Jury and D. W. Kirk, Ultimate Capacity of Steel Columns Loaded Biaxially, EIC, ER and SER 2, 1964.

8. Ellis, J. S., and P. J. Marshall, The Ultimate Capacity of Steel Columns Loaded Biaxially, Paper presented at the annual meeting of the Column Research Council, 1967.

9. Galambos, T. V., and R. L. Ketter, Columns Under Combined Bending and Thrust, Proceedings, ASCE, Vol. 85, EM 2, 1959.

10. Huber, A. W., and R. L. Ketter, The Influence of Residual Stress on the Carrying Capacity of Eccentrically Loaded Columns, Publication, Int. Assoc. for Bridge and Struc. Eng., Vol. 18, Zurich, 1958.

11. Johnson, B. G., Guide to Design Criteria for Metal Compression Members, 2nd Ed., John Wiley & Sons, Inc., New York, 1966.

12. Ketter, R. L., E. L. Kaminsky and L. S. Beedle, Plastic Deformation of Wide Flange Beam Columns, Trans., ASCE, Vol. 120, 1955.

13. Mason, R. E., G. P. Fisher and G. Winter, Eccentrically Loaded Hinged Steel Columns, ASCE, Vol. 84, EM4, 1958.

14. McVinnie, W. W., Elastic and Inelastic Buckling of an Orthogonal Space Frame, Ph.D. Thesis, Univ. of Illinois, 1966.

15. Newmark, N. M., Numerical Procedure for Computing Deflections, Moments, and Buckling Loads, Trans., ASCE, Vol. 108, 1943.

16. Ojalvo, M., Restrained Columns, Proceedings, ASCE, Vol. 86, EM5, 1960.

17. Salvadori, M. G., and M. L. Baron, Numerical Methods in Engineering, Prentice-Hall, Inc., Englewood Cliffs, N. J., 1952.

18. Sharma, S. S., Strength of Steel Columns with Biaxially Eccentric Loads, Ph.D. Thesis, Univ. of Illinois, 1965.

19. Timoshenko, S. P., and J. M. Gere, Theory of Elastic Stability, McGraw-Hill Book Co., New York, 1961.

NOMENCLATURE

a	length of a typical element of the column deflection curve
a_{ij}, a_{ji}	factors defining the length of tension or compression yield on an edge
delta	initial specified value for v and e^x
e^x, e^y	eccentricities from the x and y axes respectively
i, i+1	points on the column defection curve
i, j	corners of the edge under consideration
r^x, r^y	radius of gyration about the x and y axes respectively
u, v	lateral displacements of the shear center in the x and y directions respectively
z	coordinate along the member
A	area of the cross section
A	maximum value of delta
B	specified error in δ
B^x, B^y	bending stiffnesses about the x and y axes respectively
D	half depth of the cross section
E	modulus of elasticity
I^x, I^y	moment of inertia of the cross section about the x and y axes respectively
K	factor defining the half width of the cross section
L	column length
M^x, M^y	bending moments about the x and y axes respectively
P	axial load applied to the column
P_e	Euler load
P_y	yield load
S	**slope of line ad in Fig. 2.8**

ρ	ratio of x-moment at one column end to the x-moment at the other column end
γ	ratio of the x-moment to the y-moment at the same end of the column
δ	the deflection of i+1 from the column deflection curve at i
ϵ	strain
$\bar{\epsilon}$	bending strain
ϵ_o	uniform normal strain
ϵ_y	yield strain
θ^x, θ^y	rotations about the x and y axes respectively
θ^x_y	yield rotation
σ	stress
ϕ^x, ϕ^y	x and y axes curvatures
ϕ^x_y	yield curvature
ψ	change in slope between i and i+1 on the column deflection curve

VITA

Thomas Lawrence Scott was born in Windsor, Ontario, on March 19, 1944. He entered Assumption High School in Windsor for his secondary education in 1957. After graduating from high school in 1962, he entered the University of Windsor to study civil engineering. Mr. Scott received a Bachelor of Applied Science degree in May, 1966. In September, 1966, he continued his studies at the same university in order to obtain the degree of Master of Applied Science in Civil Engineering.

Mr. Scott is a member of the Association of Professional Engineers of Ontario and the Engineering Institute of Canada.